Heating in a reactor fuel element rod under transient conditions. Part II. DINO. Temperatures during a loss of coolant accident

Abel-Larsen, H.; Lolk Larsen, M.

Publication date:
1972

Document Version
Publisher's PDF, also known as Version of record

A. E. K. Risø

Risø - M - 1533

Risø - M - 1533

Title and author(s)

Heating in a Reactor Fuel Element Rod under Transient Conditions.

Part II. DINO.

Temperature during a Loss of Coolant Accident.

by

H. Abel-Larsen and M. Lolk Larsen

Date 12 September 72

Department or group

Reactor Engineering Department

Group's own registration number(s)

25-3-10-2

Internal report no. 355

35 pages + tables + 11 illustrations

Abstract

A computer programme to calculate the temperatures in a fuel rod subject to a loss of coolant accident is described.

The programme requires descrete information of the coolant channel hydraulic history stored on an external storage device, magnetic tape or data cards. The temperature response of the fuel rod is described in a finite difference formulation. The solution of the finite difference scheme is performed by the alternating directional implicite method, which is always stable and well suited to handle large equation systems. The programme determines the heat transfer coefficients along the channel based upon the hydraulic history and several heat transfer correlations in the programme. The heat fluxes are computed through all internal and external surfaces. The decay of power in the fuel rod during the blow down is input to the programme.

The programme is written in Algol for the Risø Borroughs B6700 computer. Plotter procedures are widely used to finish the output and lineprint output is minimized. The problem size, i.e. the number of nodes, is independent of the programme, only determined by the user. The ratio procestime/real time for a 500 node problem is 100:1.

Copies to

Abstract to

Available on request from the Library of the Danish Atomic Energy Commission (Atomenergikommissionens Bibliotek), Risø, Roskilde, Denmark.
Telephone: (03) 35 51 01, ext. 334, telex: 5072.

Fi 25-204

CONTENTS

LIST OF FIGURES

1. INTRODUCTION

The analytical prediction of core temperatures, pressures and forces during a postulated reactor accident such as a loss of coolant accident, is an important part of the estimation of the safety, which is inherent and engineered into a given reactor system.

The loss of coolant accident based on the assumption of a circumferential rupture with unobstructed discharge from both ends of the largest pipe is assumed to be the max. credible accident in a BWR and PWR. The rupture results in a fast system decompression, which partly exposes the inner core structure to great forces and partly releases the latent energy in the water resulting in a fast increase in the steam formation.

Even if the nuclear scram system is functioning a considerable heat energy is left in the core due to the capacity and the decay of fission products. This heat energy must be removed in order to avoid melting of the core. Further the increase in the canning temperature must be limited in order to avoid metal-water reaction, which is exotermic and may be an essential source of heat.

The cooling problems will be complicated considerably, if the core configuration is changed in consequence of the influence of forces and melting of the core. It is assumed in what follows, that the core configuration is unchanged during the accident.

The use of digital computers allow very comprehensive calculations, but still there exist limits on the degree of details to be achieved and the physical phenomena to be represented. In order to reduce the uncertainties connected to these limitations it has been considered advantageous to divide the analysis into three parts:

A: Analysis of the blow down, limited to the calculation of the system decompression, system flows, discharge flows and influence of forces upon the inner core structure during the loss of coolant accident.

B: Analysis of the temperature transient in a single fuel rod during the blow down taking into consideration enthalpy increase, burn out and heat transfer to the coolant channel.

C: Analysis of the temperature transient in the fuel after the blow down taking into consideration thermal radiation heat transfer with multiple reflection between solid surfaces, heat transfer to emergency core coolant and metal water reactions.

The analysis of the blow down is performed with the hydraulic programme BRUCH-S/1/, while the temperature response to the blow down is computed by the core heat up programme DINO, described in this report. These two programmes are linked together by a data-coupling technique, using an external computer storage device. This method gives a great degree of freedom, as the two programmes can be run independent of each other. Many changes in programme structure can be done and basic improvements in the programme theory may be tested without affecting the data-coupling, so each programme can still be considered as a separate unit. DINO is not restricted to one blow down programme, but can be used in connection with other programmes describing blow down in both BWR and PWR systems. The only restriction is that the information required for processing in DINO is obtainable from the programme.

The analysis of the temperature transient after blow down is performed with the computer programme REMI/HEATCOOL /2/.

The object of DINO is to calculate the cladding and fuel pellet temperatures during the blow down of a loss of coolant accident. The programme uses the blow down information to calculate the heat transfer coefficients. The integration of the temperatures is performed only on the solids.

2. CORE HEAT UP IN THE BLOW DOWN PERIOD

The blow down period is characterized by the strong transient flow, which makes the determination of the heat transfer coefficients problematic.

However, by using finite difference methods,the time history of the blow down may be considered as quasistationary with reasonable accuracy. Unlinearities from the temperature dependent parameters such as heat conductivities, heat capacities etc. can be taken into account, when the timesteps are chosen sufficiently small. Heat

transfer coefficients calculated from correlations obtained from stationary conditions are assumed to be applicable.

The core heat up programme DINO is a two dimensional, transient finite difference programme, which is based upon the above-mentioned principles. The time history of the blow down is divided into phases, which are determined by the flow conditions taken from the blow down programme BRUCH-S:

1. phase is the first short time period, where nucleate boiling still is prevalent.

2. phase starts, when dryout occurs, but the surface temperature is lower than the Leidenfrosttemperature, and the surface is still accessible to direct water cooling; this is the transition cooling phase.

3. phase is characterized by the dryout, and the surface temperature is higher than the Leidenfrost temperature i.e. the surface is coated with a superheated layer of vapour.

The loss of coolant accident includes a 4. phase, the thermal radiation phase. When the pressure in the reactor vessel and the containment is largely equalized and the convective heat transfer is reduced so much that the thermal radiation is dominating in the overall heat transfer process the calculations may be continued by the computer program REMI/HEATCOOL.

3. GEOMETRIC MODEL

The main object of DINO is to calculate the cladding and fuel pellet temperatures as function of time during the blow down period, i.e. during the phases 1, 2 and 3.

Only a single rod is considered. The influence of the surrounding rods and shroud is taken into account as the outer wall of an annulus with an equivalent amount of fuel and cladding.

The necessary and sufficient degree of detailled information

is secured in this way, and relevant phenomenas can be included in the programme. The design of a BWR fuel element requires 3 different locations of rods to be considered in the calculations in order to cover the complete element, i.e. corner rod, side rod and central rod as shown in fig. 1. Fig. 1 also shows the assumed boundaries of the surrounding rods and shroud.

It is assumed that the equivalent diameter concept is valid:

$$DEKV = \frac{4 \times ACAF}{ACHTA}$$

where

ACAF is the actual flow area connected to the considered rod as defined above and shown in fig. 1.

and

ACHTA is the actual heat transfer area connected to the considered rod.

The equivalent single channel is then determined so that the ratio between the actual equivalent diameter DEKV and the equivalent diameter of the model is unity

$$DEKVM = \frac{4 \times AFLOW}{EQHTA} = DEKV.$$

AFLOW is the equivalent flow area and EQHTA is the equivalent heat transfer area. Referring to fig. 2 DEKVM may be written

$$DEKVM = DIS - DROD.$$

As the dimensions of the considered rod are retained, the inner diameter of the outer wall DIS can be calculated. The equivalent flow area AFLOW and the equivalent heat transfer area EQHTA can be calculated. The ratio

$$\frac{ACAF}{ACHTA} = \frac{AFLOW}{EQHTA}$$

may be rewritten to

$$\frac{ACAF}{AFLOW} = \frac{ACHTA}{EQHTA},$$

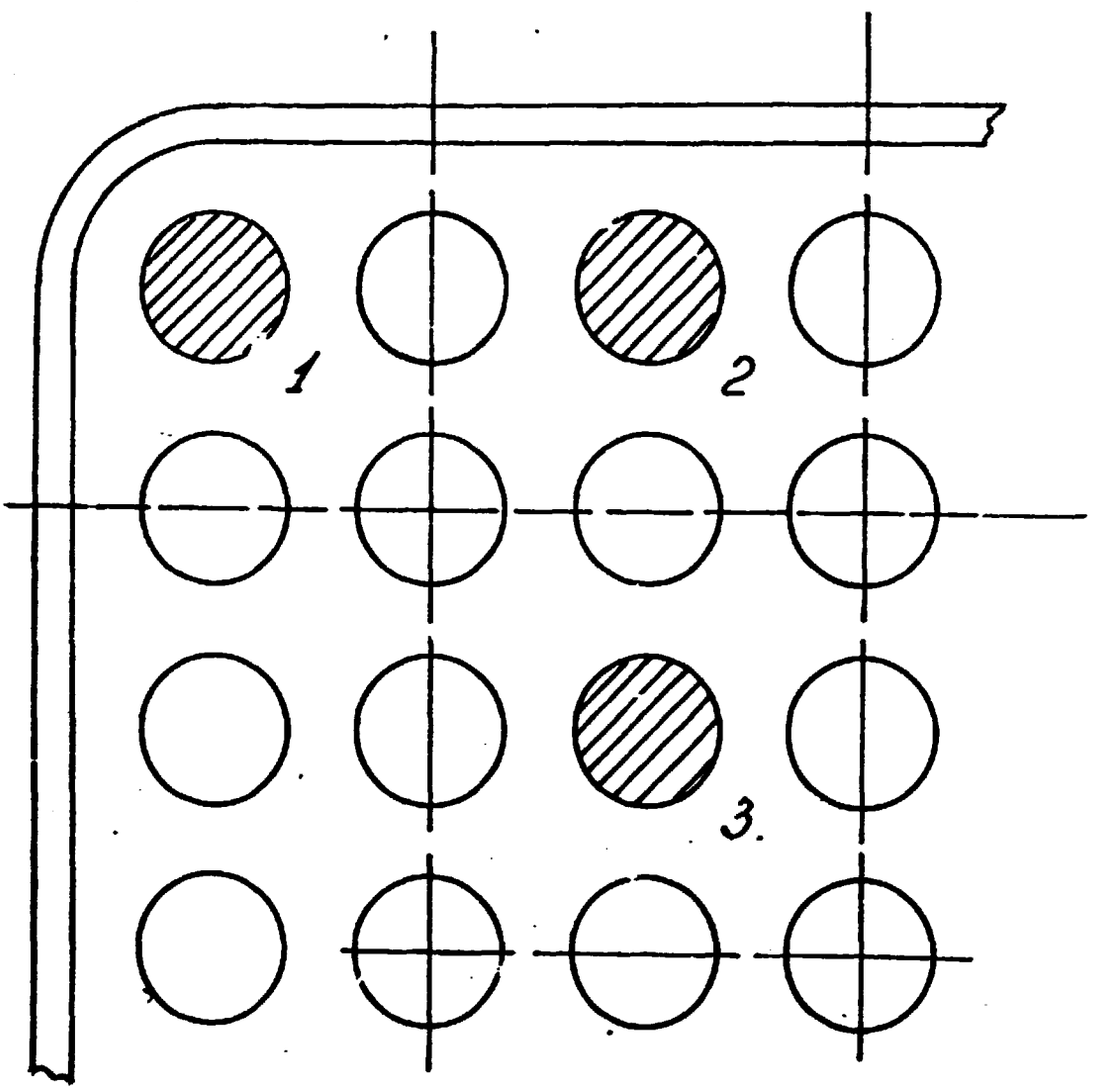

Fig. 1

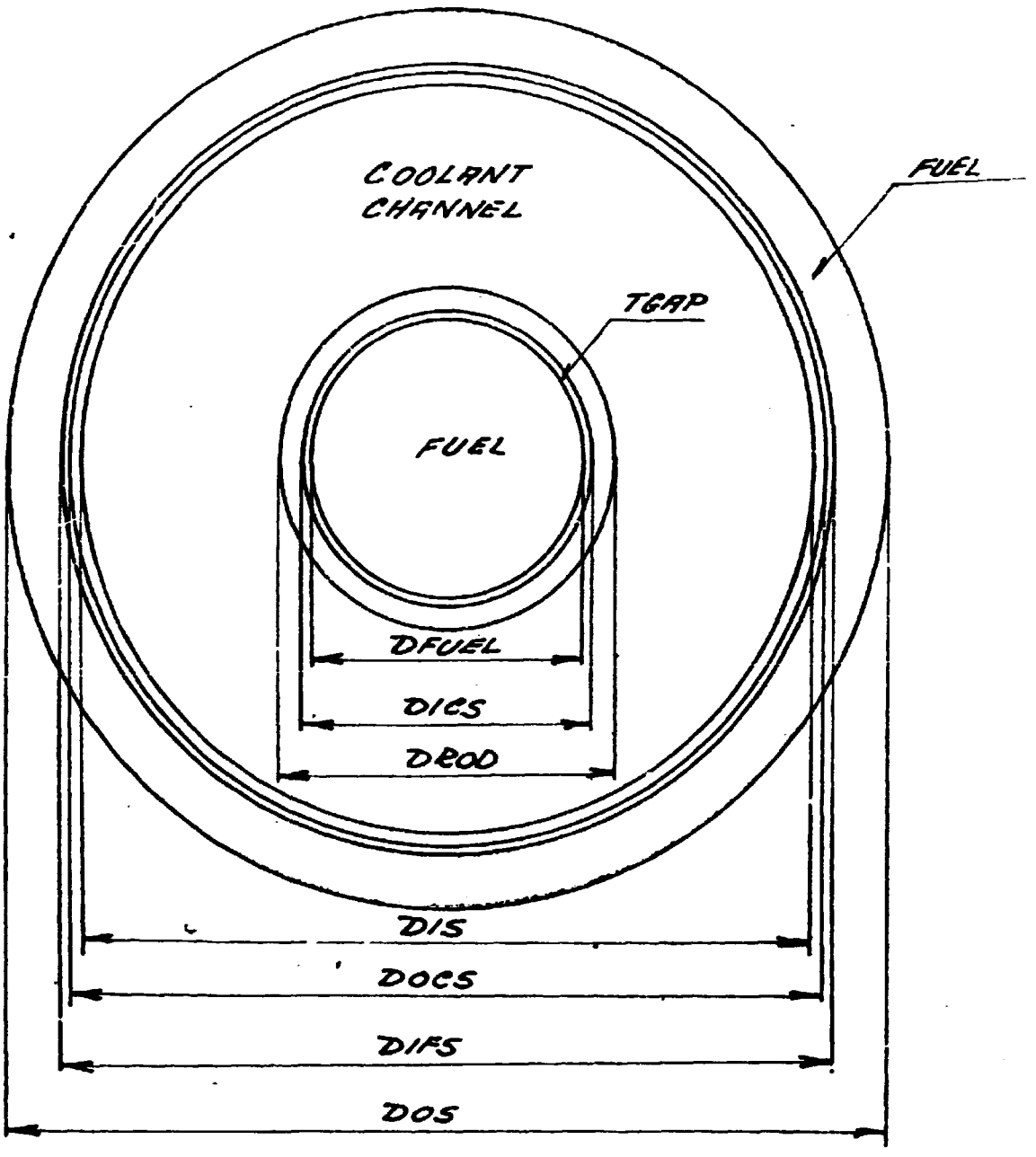

EQUIVALENT SINGLE CHANNEL.

Fig. 2

i.e. the actual heat transfer area is reduced with the ratio AFLOW/ ACAF. This ratio must therefore be retained in the calculation of the equivalent heat generating area and the equivalent cladding area.

For the heat generating areas we have:

$$\frac{AHGA}{EQHGA} = \frac{ACAF}{AFLOW}$$

where AHGA is the actual heat generating area and EQHGA is the equivalent heat generating area. For the cladding areas we have:

$$\frac{ACLA}{EQCLA} = \frac{ACAF}{AFLOW}$$

where ACLA is the actual cladding area and EQCLA is the equivalent cladding area.

Do we use the same mass flux in the equivalent system as in the actual system, the Re-number will be the same in the two systems. The considered rod retains its dimensions i.e. the reduction goes on the outer wall of the annulus, which means, that less heat is generated here, but as the flow area is reduced in the same ratio the enthalpy of the coolant will be the same. The Pr-number and the other parameters determining the heat transfer coefficient will be the same. This is of course based on the assumption, that cross flow and mixing in the actual geometry are negligible. The dimensions of the geometric model, the equivalent single channel, for the 3 possible placings can thus be calculated.

Fig. 2 shows the equivalent geometric model used.

4. INTERACTION BETWEEN FUEL RODS AND COOLANT

The interaction between fuel rods and the coolant is complicated to compute due to the large difference in propagation of change in the different media. Under the assumption of a fixed power in the rods, the coolant channel mainly determines the temperature response of the rod, and the effect of the rods on the coolant channel is of

second order. When this interaction is described in finite differences, the transient behaviour of the coolant channel therefore determine the number of integration steps needed to compute temperature changes, as each step requires fixed boundary conditions, i.e. constant heat transfer coefficients. To achieve a fast programme the philosophy behind the structure is:

The programme is divided into two main parts, a heat conduction model and a channel thermal hydraulic model. The coolant channel and the fuel rod is treated independant of each other in a small time increment assuming constant boundary conditions. The coolant temperatures and heat transfer coefficients are determined from the coolant channel data. The only integration to perform is the temperature distribution in the solids. When the temperatures are computed, the two parts of the problem are related by the conservation of energy for each time increment ("radiation condition").

Each integration step length is determined by the change of the heat transfer coefficient. When the change of heat transfer coefficients in the channel is small a large integration time step can be used, but when the variation in the coolant channel is strong only small time steps are valid.

"The radiation condition" may be violated if too large a change of heat transfer coefficient is allowed during the determination of the time step. The allowable change of the heat transfer coefficients during the search for the time step length is specified by the user.

4.1 Heat conduction model

A detailled description of the heat conduction model is given in /3/. The transient two dimentional heat conduction equation

$$\frac{\partial}{\partial x}\left(k_x \frac{\partial T}{\partial x}\right) + \frac{\partial}{\partial y}\left(k_y \frac{\partial T}{\partial y}\right) + q'''(x, y) = \rho c_p \frac{\partial T}{\partial t}$$

where

k_x, k_y	heat conductivity in x and y direction	Watt/m ^oC
T	temperature	^oC
q'''	volumetric heat generation	Watt/m^3
ϱ	density	kg/m^3
c_p	heat capacity	Joule/kg ^oC
t	time	sec.

is solved in a rectangular geometry by the ADI-method /4/. This method implies, that the solution is approximated by finite differences. The problem is subdivided into nodes by a grid, from which the program derives the finite differences. The grid is specified by input quantities and the grid size is completely independent of the program. The applied geometry is restricted to cylindrical coordinates, using the Max Jacob transformation.

Tne ADI-method has several advantages over normal finite difference formulations:

1) The method is always stable, i.e. the user can specify the size of the time steps.

2) The neccessary computer storage is low. If the initial temperatures are contained in the array T /0:N, 0:M/, only three additional arrays of the size TT /0:N, 0:M/, X, Y/ 0:P/ where P = N,M are needed to store intermediate results during the solution of the finite difference equations.

3) The solutions of the finite difference equations are simple and straight forward. The algorithm is of the type

$$T_{N-1} = Y_{N-1}$$

$$T_r = Y_r - X_r \times T_{r+1} \qquad 0 \leq r \leq N-2$$

4.1.1 Effective conductivities

The local heat conductivities within the nodes are temperature dependent. Every time an integration is performed, all local

conductivities are reevaluated, based on the just computed temperature distribution. The effective conductivities between all neighbouring nodes, both in radial and axial direction, are determined from the local conductivities, using the balance of heat between any two related nodes /3/. This implies that the temperature distribution between each step is considered constant. Effective conductivities between nodes separated by a gas gap, or nodes separated by a solid/coolant interface is computed in a similar manner, using the balance of heat /3/. The thermal radial radiation is computed between all internal opposite surfaces. For the applied geometry all viewing factors are assumed unity. Radiation is included in the relevant effective conductivities.

4.1.2 Gas gap heat transfer

A gap between the fuel pellets and the cladding inner surface is not treated as a single node but it is assigned to a grid boundary. The size of the gap is constant throughout the computation. The variable gas gap size and the changing heat transfer coefficients in the gap is taken into account by use of a special formula.

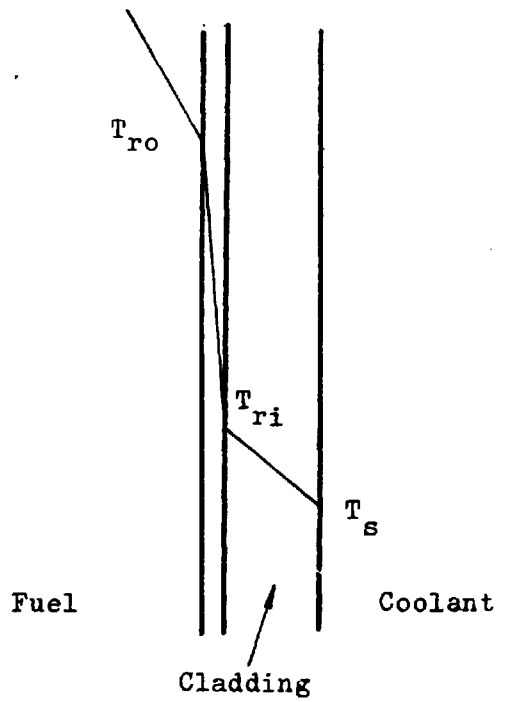

Fig. 3

The controlling temperature T_{gap} for the gap heat transfer is determined from:

$$T_{gap} = \frac{1}{2} (T_{ro} + T_{ri}) - T_S$$

T_{ro} fuel surface temperature
T_{ri} inner cladding surface temperature
T_S outer cladding surface temperature

The relation between T_{gap} and the gas gap heat transfer h_{gap} is shown in fig. 4. The curve represents steady state heat transfer.

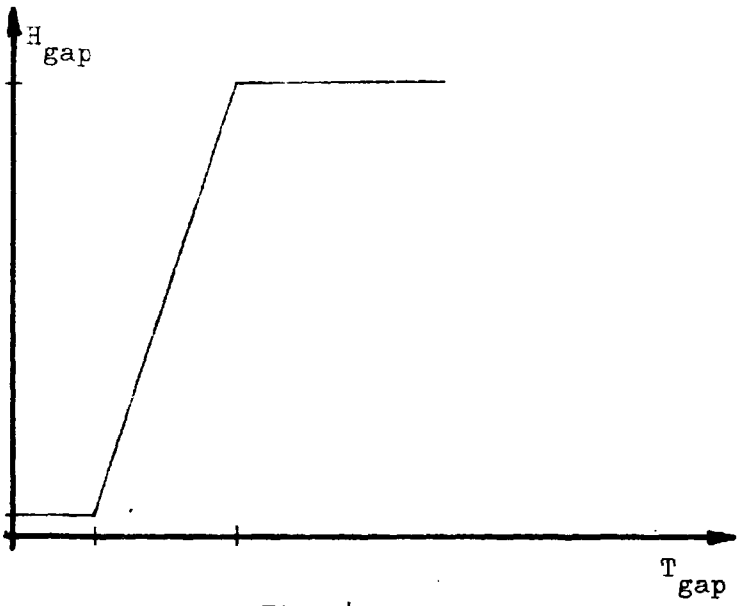

Fig. 4

The maximum value of h_{gap} is $1.2 10^4$ Watt/m^2 °C, which corresponds to maximum contact pressure between cladding and fuel. The minimum value of h_{gap} corresponds to maximum gap width and pure gas conductivity. The function $h_{gap} = h_{gap} (T_{gap})$ is based on results from the cladding-temperature-stress program TEMPDIST /5/.

TEMPDIST computes the gas gap heat transfer coefficient due to variation in gas gap width. The gas conductivity is assumed constant 1.4×10^{-2} Watt/m °C, and the gap width is determined from

thermal expansion of fuel and cladding. When the gap width becomes zero, the contact pressure is computed. The function h_{gap} (T_{gap}) is based on a constant pressure difference between gas and coolant, so no reduction in coolant pressure due to blow down is taken into account.

4.2 Coolant channel model

The coolant channel model in DINO is one-dimentional. It consists of a stack of nodes, where the axial mesh is determined by the nodal grid. The radial mesh is the annulus width. The heat transfer to the coolant channel is purely radial. Two phase slip flow is not taken into account in the present version of DINO. DINO is supplied with blow down data from the hydraulic programme BRUCH-S.

For each node BRUCH-S computes the pressure, mass and enthalpy. In the links between the nodes the mass flows are computed. The information relevant to DINO is:

1. transient time
2. pressure in the core
3. mass flow and enthalpy at the inlet to the core
4. mass flow at the outlet from the core.

The core pressure is considered constant over the entire core length. The mean mass flow through the core is computed from: $G_{mean} = 0.5 (G_{in} + G_{out})$, and is considered constant throughout the core. The direction of the flow is in BRUCH-S indicated by a sign. Normal flow direction i.e. direction of flow during steady state operation is positive and reversed flow is negative. This rule is adopted in DINO.

The mass flux is assumed constant over the total core inlet area and it is computed from BRUCH-S as:

$$G_{flux} = G_{mean}/A_{inlet} \quad \text{where } A_{inlet} = \text{total core inlet area.}$$

The following quantities are computed in DINO at each level of the coolant channel: enthalpy, steam quality, coolant temperature and heat transfer coefficient.

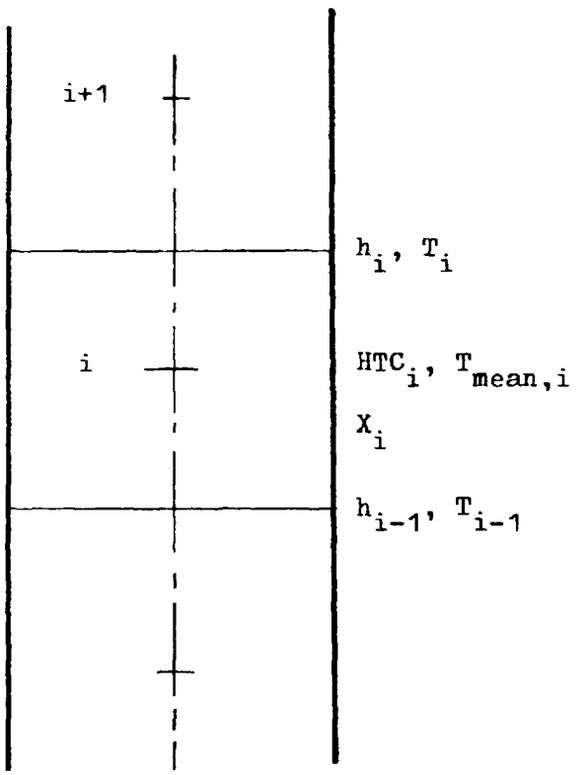

Fig. 5

The enthalpy is computed in the outlet from each node, based upon a steady state energy balance. The steam quality in a node is computed from the mean enthalpy between node inlet and node outlet and coolant channel pressure. If the node is saturated, the node temperature is that of the saturation pressure. If the node is subcooled the node outlet temperature is computed from the outlet enthalpy and heat capacity as function of pressure and subcooling temperature. The temperature assigned to a node is the mean between inlet and outlet temperatures. Finally the heat transfer coefficient is computed in each node.

4.2.1 Heat transfer coefficients

The time history of the blow down may be divided into 3 phases, as mentioned above.

Nucleate boiling is prevalent in the first phase. The heat transfer coefficient is determined by use of the Thom's formel /6/

$$\Delta T_{THOM} = T_S - T_{SAT} = 2.252 \times 10^{-2} \times q''^{0.5} \times \exp.(-1.1511 \times 10^{-7} \times p),$$

$$h_{NB} = q''/\Delta T_{THOM}$$

where

T_S is the surface temperature (^oC)

T_{SAT} is the saturation temperature at the prevalent pressure (^oC)

q'' is generated heat flux (Watt/m^2)

p is the pressure (N/m^2)

h_{NB} is the heat transfer coefficient (Watt/m^2 ^oC).

The transition from the first phase to the second phase is determined by the dryout. Bertoletti's correlation /7/ is used in the first version of DINO.

$$X_{crit} = \frac{(1 - p/p_c)}{(0.1 \times G^{0.33})} \times \frac{L_B}{L_B + 0.19875 \times D_H^{1.4} \times G \times (p_c/p-1)^{0.4}}$$

where

X_{crit} is the critical steam quality (dim. less)

p is the prevalent pressure (N/m^2)

p_c is the critical pressure (221.29×10^5 N/m^2)

G is the mass flux ($kg/m^2 sec.$)

L_B is the boiling length (m)

D_H is the hydraulic diameter (m).

Dryout occurs, when the critical steam quality is less than the calculated local steam quality. Immediately after dryout it is still possible for the coolant to wet the cladding surface and the heat transfer coefficient may be higher than that, determined by film boiling. Experiments show an oscillating surface temperature indicating partly wetting of the surface and partly a coating of the surface with superheated vapour. Only few experiments on the transition area have been published and the results scatter very much.

We have assumed in the first version of DINC, that the Leidenfrost temperature may be used as indication of whether we are in the transition cooling phase or in the film boiling phase. The Leidenfrosttemperature is a function of pressure, material and surface roughness. On the basis of examinations carried out by Bennet et al., AERE-R-5146 (1966), Parker and Grosh, ANL-6291 (1961) and Bertoletti et al., CISE R-36 (1961) the following best estimate of the Leidenfrosttemperature as function of the pressure is:

$$\Delta T^{-1} = (T_{WLEI} - T_{SAT})^{-1}$$

$$= 9.0945 \times 10^{-3} + 3.6963 \times 10^{3} \times p^{-1}$$

where p is the pressure (N/m^2). Is the surface temperature less than the Leidenfrosttemperature the transition cooling is prevalent. Due to lack of reasonable supported correlations in this regime a purely empirical equation for the heat transfer coefficient has been developed. The heat transfer coefficient in this regime must have a value between the heat transfer coefficient determined by the THOM-correlation and the heat transfer coefficient determined by the film boiling. Further it must be reasonable to assume, that the nearer the surface temperature is the THOM-temperature the nearer the heat transfer coefficient will correspond to that of nucleate boiling and vice versa. Based on this, the following equation has been set up:

$$h_{TB} = h_{FB} \left(1 + 0.01^{n} \times (h_{NB}/h_{FB} - 1)^{1-n}\right)$$

where

h_{TB} is the heat transfer coefficient corresponding to the transition regime,

h_{FB} is the heat transfer coefficient corresponding to the film boiling regime,

h_{NB} is the heat transfer coefficient corresponding to the nucleate boiling regime,

n is an exponent, which is determined from the equations.

$$n = \frac{T_S - T_{WTHOM}}{T_{WLEI} - T_{WTHOM}}$$

where

T_S is the actual surface temperature,

T_{WTHOM} is the surface temperature determined by THOM's correlation,

T_{WLEI} is the Leidenfrosttemperature determined from the above mentioned equation.

The programme uses n = 0.1 if n is calculated to be less than 0.1. Parker and Grosh /8/ have found, that the heat transfer coefficient in the transition regime may be 6-7 times better than the film boiling coefficient. The equation agrees with this result. Further the equation has been compared with the CISE-results and good agreement has been found especially by smaller n, but with n near 1 the agreement fails. This is without no doubt due to inaccuracies in the equation for the Leidenfrosttemperature. Here again it must, however, be borne in mind, that the equation is purely empirical and experiments are necessary.

With the surface temperature beyond the Leidenfrosttemperature pure film boiling is assumed to be prevalent. The heat transfer coefficient in the film boiling regime is in the first version of DINO determined from the correlation

$$h_{FB} = 0.020 \times \frac{k}{D_e} \times (Re)^{0.8} \times (Pr)^{0.4} \times \left(\frac{T_{SAT}}{T_{WALL}}\right)^{0.5}$$

USAEC's interim criteria claims the Groeneveld's correlation /9/ to be used:

$$h_{FB} = 5.20 \times 10^{-2} \times \frac{kg}{D_H} \times \left[Re_g \left(X + \frac{\varrho_g}{\varrho_l}(1-X)\right)\right]^{0.688} Pr_W^{1.26} \times Y^{-1.06}$$

ϱ_g and ϱ_l are the mass densities for steam and water respectively,

Pr_W is the Prandtl's number determined for saturated water, and

$Y = 1 - 0.1 \times \left(\frac{\varrho_l}{\varrho_g} - 1\right)^{0.4} \times (1 - X)^{0.4}$.

The last correlation is more conservative than the first mentioned.

4.2.2 Time step size

The variation of the heat transfer coefficients with time determine the size of the time step to be used for the integration in the solids. The hydraulic information produced by a blow down programme will be available as a sequence of data sets, where each data set describes the hydraulic state at a fixed time. Normally the time increment between successive data sets are small, and it is therefore advantageous to gather several data sets in one large time step to decrease the total number of integrations required by the complete problem.

According to each data set a computation of the heat transfer coefficient is performed in each axial level of the channel. When this has been done for more than one data set, a test in each level of the variation between successive heat transfer coefficients takes place. The relative difference between these coefficients are stored. If all levels accept the test, a new data set will be supplied to the program, and a new computation of the heat transfer coefficients HTC are performed. These are again tested against the just computed heat transfer coefficients HTC^1, and the relative difference:

$A = \frac{HTC - HTC^{1}}{HTC^{1}}$ is added to the previous one for each level.

If the total change in just one level exceeds a present band width, the time increment is computed for the HTC's contained in that band, (see fig. 6). A mean heat transfer coefficient is computed for each axial level, and the integration takes place, using the just computed time step. The mean heat transfer coefficients are assigned to the middle of this step. If the band width is not exceeded more data sets are supplied, until the band width is broken. A maximum number of 50 data sets are allowed to be gathered in one time step, if the band width is not exceeded at least once.

When the integration has been performed, and the programme returns to the search for the next time step, the level for the new band is determined by the last heat transfer coefficient contained in the old band. This means, that the actual band will have an area common with both the previous and the next band. This method assure that steps between successive mean heat transfer coefficients are less than the band width.

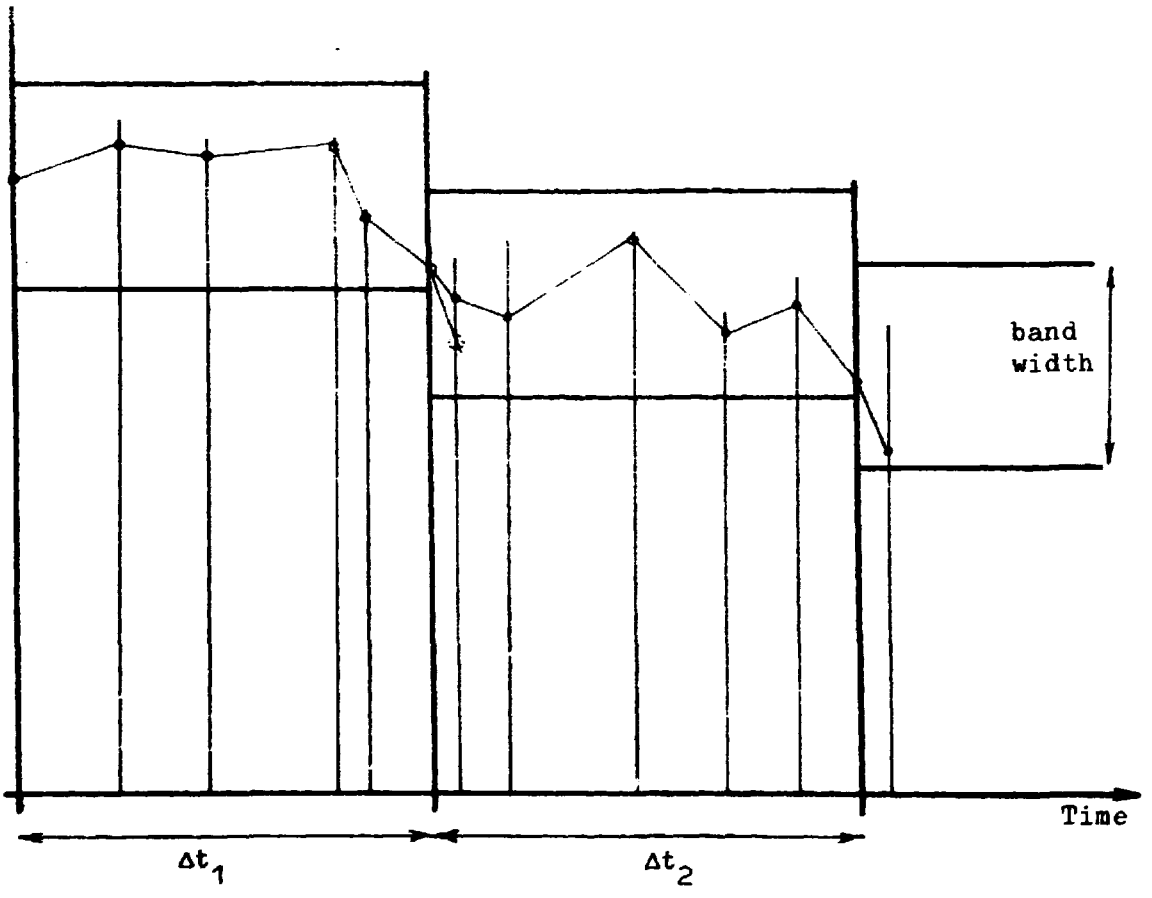

Fig. 6

4.2.3 Heat fluxes

The heat fluxes through all internal surfaces are computed after each integration, using the just determined temperatures and the effective conductivities, assigned to the middle of the time step.

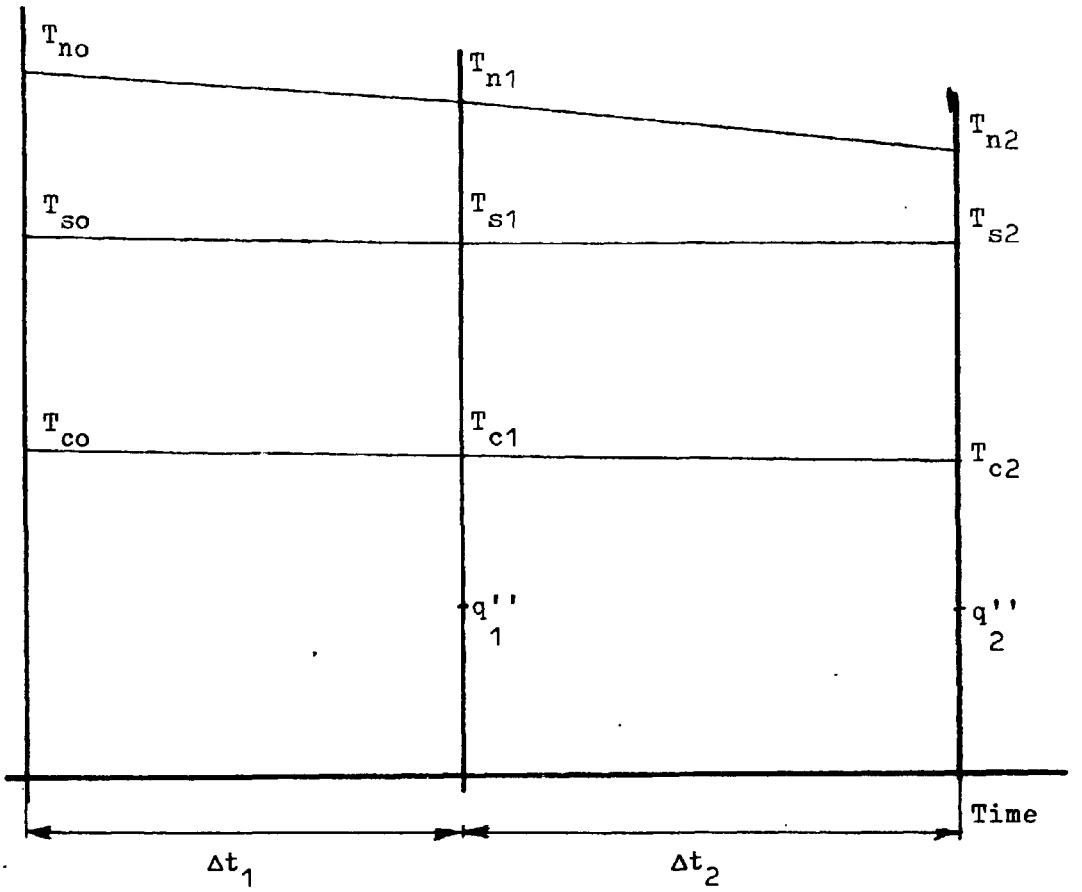

Fig. 7

T: temperature
h: mean heat transfer coefficient
K: effective heat conductivity
q'': surface heat flux
n: cladding node
s: cladding surface
c: coolant node
Δx: distance between nodes

These heat fluxes are assumed constant during the search for the new time step. The heat flux in a particular level is computed from: (see fig. 7)

$$q_1'' = (T_{n1} - T_{c1})\ K_1/\Delta x$$

The formulas applied in the programme assure, that the following equation is fulfilled at time t:

$$q_1'' = h_1\ (T_{s1} - T_{c1})$$

At time t + Δt the flux is computed from:

$$q_2'' = (T_{n2} - T_{c2})\ K_2/\Delta x$$

Small increments between successive quantities - temperatures or heat fluxes - characterize a proper computation using a finite difference formulation, and the time step applied in the integration must therefore be controlled to assure this result. The time step chosen must take into account possible strong unlinear loops in the programme structure and the transient behaviour of the considered problem.

The band width assures,that the difference between a heat transfer coefficient and the corresponding mean heat transfer coefficient is fixed. A small band width results in a small difference.

The necessary and sufficient conditions to assure a proper result with DINO are:

1. a reasonable small band width,
2. an upper limit of the time steps.

The upper limit of the time steps is obtained by experience, and in the present version of DINO, it is fixed to 0.1 sec.

If the computed heat transfer coefficients in a period became constant, theoretically a very large time step might be computed. In practice, however, the heat transfer coefficients always change and a very small band width will assure a proper computation, by

keeping the time steps small. To obtain a programme speed close to optimum, we have chosen to play both on band width and max. time step.

The heat flux computation may involve a strong unlinear loop in the programme dependent on the applied heat transfer correlations. The heat transfer correlations applied in the present version of DINO do not contribute to an unlinear programme loop. This result is easily seen from figure 19.

4.2.4 Flow chart for the thermal hydraulic model

The thermal hydraulic part of DINO is modelled in one procedure, that contains the total control of the thermal hydraulic computation. The procedure receives from the main programme the just computed temperature distribution in the problem, and it feeds back the size of the next time step. The procedure also returns the mean heat transfer coefficient and the coolant temperature for each level connected with that time step. The procedure calls subprocedures, which compute the heat transfer coefficients or the physical properties of water. A detailled description of the procedure is given by the flow chart on page 23 and 24.

The procedures applied in the flow chart are:

1) Physical properties of water:

TP(p) : Saturation temperature as function of pressure p

h(TP) : Saturation enthalpy as function of saturation temperature TP

R(p) : Heat of evaporation as function of pressure p

CP(p, T(J)) : Subcooled heat capacity as function of pressure p and temperature T(J) at level J.

2) Heat transfer correlations:

HC(p,MFLUX,TE(J)): One phase heat transfer coefficient at level J as function of pressure p, mass flux in channel MFLUX, and coolant temperature TE(J) in level J

HNB (QPROP(J),p) : Nucleate boiling heat transfer at level J as function of heat production QPROP(J) in level J and pressure p

HFB(MFLUX,TS(J)) : Film boiling heat transfer at level J as function of mass flux and surfacetemperature TS(J).

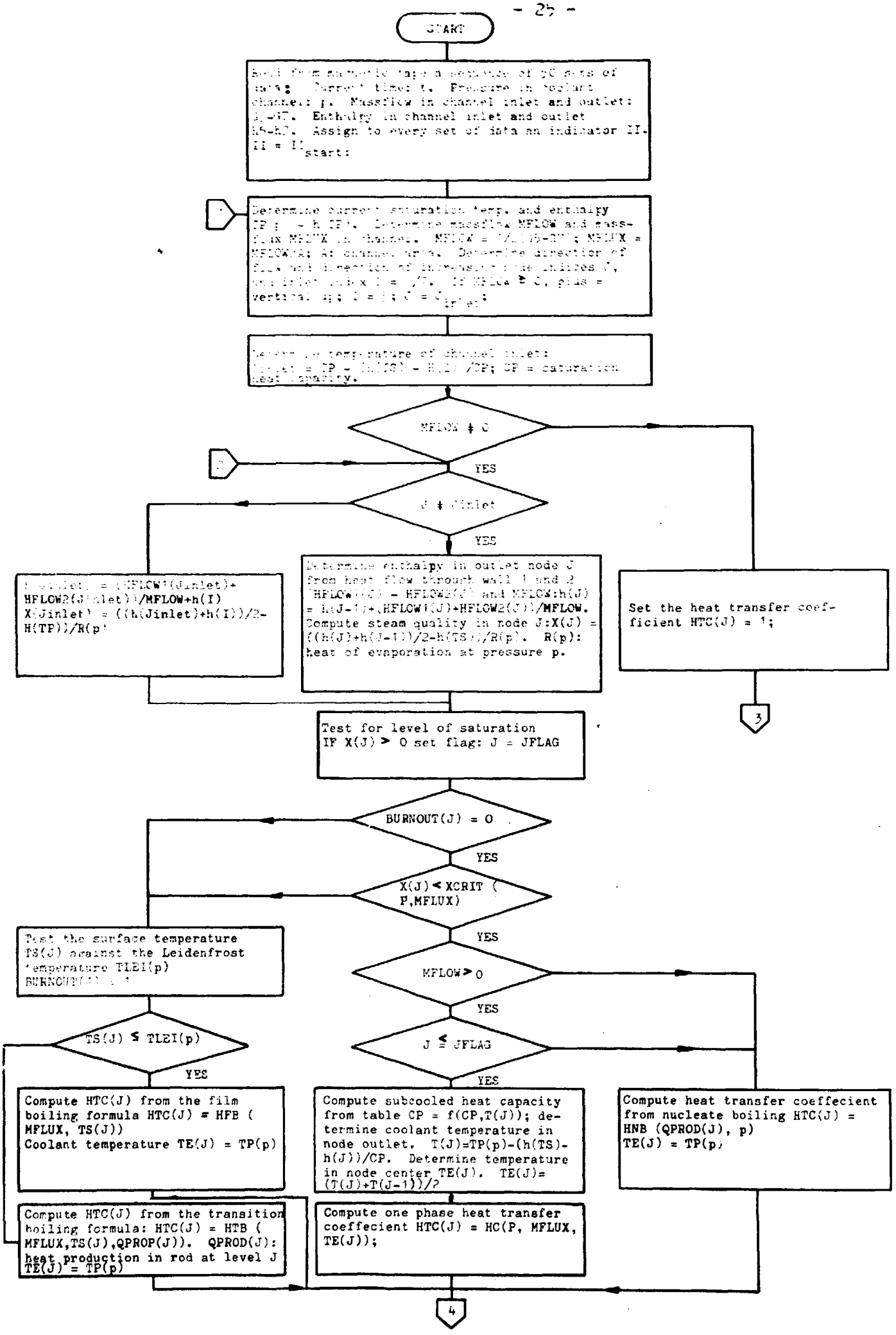
START
Read from memory: tape a set/case of 20 sets of data: 'Burn' time: t. Pressure in coolant channel: p. Massflow in channel inlet and outlet: h5-h7. Assign to every set of data an indicator II. II = II start:
Determine current saturation temp. and enthalpy TP ; - h TF'. Determine massflux MFLOW and mass-flux MFLUX in channel. MFLOW = ; MFLUX = MFLOW/A; At channel area. Determine direction of flow and direction of increasing node indices J, initial value J = . If MFLOW ≥ 0, flow = vertical up; I = 1 ; J = J inlet
Determine the temperature of channel inlet: Jinlet = TP - (h(I) - H.I) /CP; CP = saturation heat capacity.
MFLOW ≠ 0
YES
J ≠ Jinlet
YES
Jinlet = ((HFLOW1(Jinlet)+HFLOW2(Jinlet))/MFLOW+h(I)
X(Jinlet) = ((h(Jinlet)+h(I))/2-H(TP))/R(p)
Determine enthalpy in outlet node J from heat flow through wall 1 and 2 HFLOW1(J) = HFLOW2(J) and MFLOW:h(J) = h(J-1)+(HFLOW1(J)+HFLOW2(J))/MFLOW. Compute steam quality in node J:X(J) = ((h(J)+h(J-1))/2-h(TS))/R(p). R(p): heat of evaporation at pressure p.
Set the heat transfer coefficient HTC(J) = 1;
3
Test for level of saturation IF X(J) > 0 set flag: J = JFLAG
BURNOUT(J) = 0
YES
X(J) < XCRIT (P,MFLUX)
YES
Test the surface temperature TS(J) against the Leidenfrost temperature TLEI(p)
BURNOUT(J) = 1
MFLOW > 0
YES
TS(J) ≤ TLEI(p)
YES
J ≤ JFLAG
YES
Compute HTC(J) from the film boiling formula HTC(J) = HFB (MFLUX, TS(J))
Coolant temperature TE(J) = TP(p)
Compute subcooled heat capacity from table CP = f(CP,T(J)); determine coolant temperature in node outlet. T(J)=TP(p)-(h(TS)-h(J))/CP. Determine temperature in node center TE(J). TE(J)= (T(J)+T(J-1))/2
Compute heat transfer coeffecient from nucleate boiling HTC(J) = HNB (QPROD(J), p)
TE(J) = TP(p)
Compute HTC(J) from the transition boiling formula: HTC(J) = HTB (MFLUX,TS(J),QPROP(J)). QPROD(J): heat production in rod at level J
TE(J) = TP(p)
Compute one phase heat transfer coeffecient HTC(J) = HC(P, MFLUX, TE(J));
4

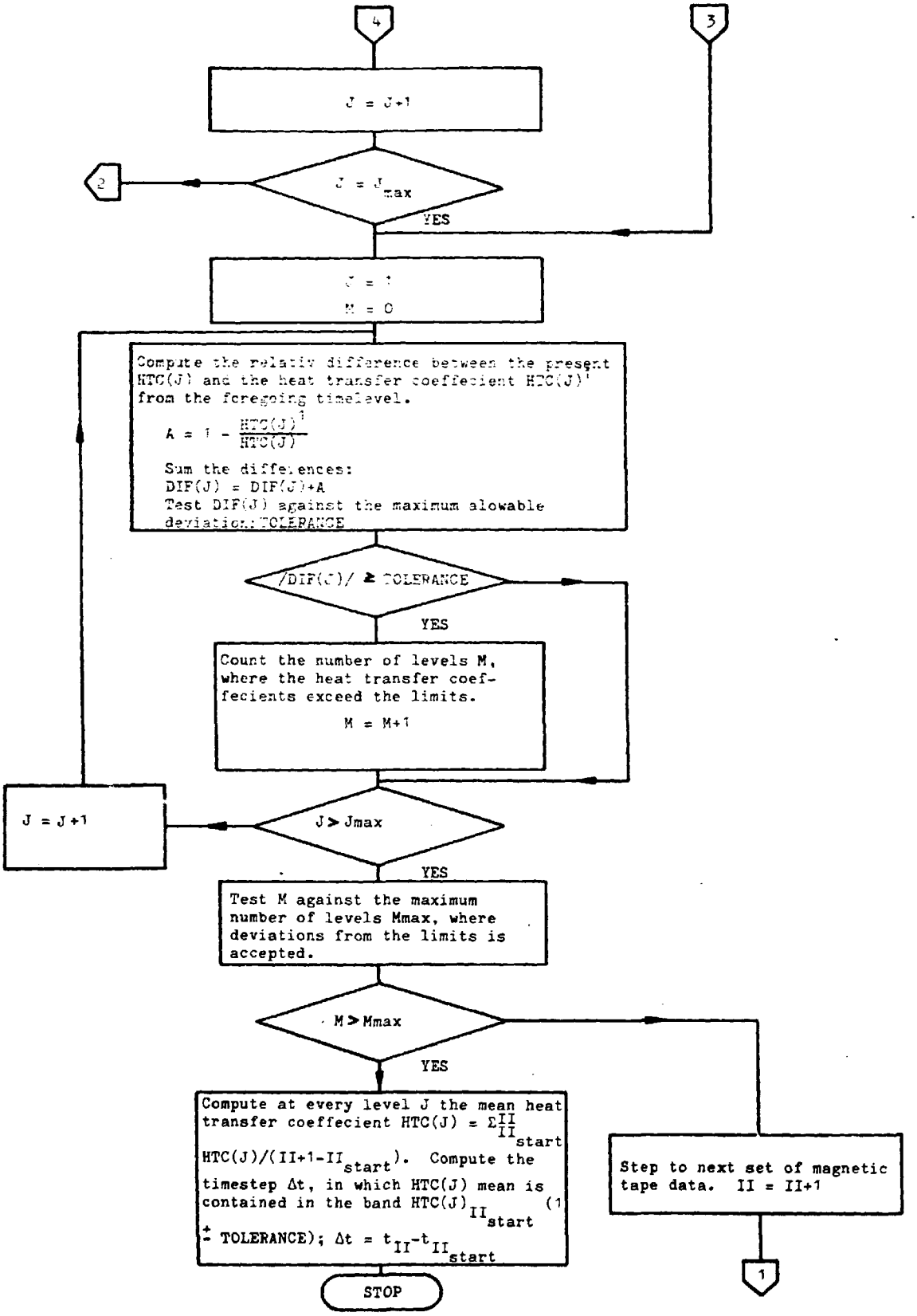
4
3
J = J+1
2
J = Jmax
YES
J = 1
M = 0
Compute the relativ difference between the present HTC(J) and the heat transfer coeffecient HTC(J)' from the foregoing timelevel.
A = 1 - HTC(J)'/HTC(J)
Sum the differences:
DIF(J) = DIF(J)+A
Test DIF(J) against the maximum alowable deviation: TOLERANCE
/DIF(J)/ ≥ TOLERANCE
YES
Count the number of levels M, where the heat transfer coeffecients exceed the limits.
M = M+1
J = J+1
J > Jmax
YES
Test M against the maximum number of levels Mmax, where deviations from the limits is accepted.
M > Mmax
YES
Compute at every level J the mean heat transfer coeffecient HTC(J) = Σ II start II HTC(J)/(II+1-II start). Compute the timestep Δt, in which HTC(J) mean is contained in the band HTC(J) II start (1 ± TOLERANCE); Δt = t II - t II start
STOP
Step to next set of magnetic tape data. II = II+1
1

HTB(MFLUX,TS(J),QPROP(J)): Transition boiling heat transfer at level J as function of mass flux MFLUX, surface temperature TS(J) at level J, and heat production QPROP(J) at level J

TLEI(p) : The Leidenfrosttemperature as function of pressure p

XCRIT(p,MFLUX) : The burnout quality as function of pressure p and mass flux MFLUX.

5. TEMPERATURE DEPENDENT PHYSICAL PROPERTIES

The temperature and time dependent thermo-physical properties of solids and coolants in DINO, introduce an unlinarity in the computation, which is handled in a quasilinear mode.

The basis for this mode is knowledge of the next time step Δt to be used. In general the time and temperature dependent properties are computed at time $t + 1/2\ \Delta t$ from the temperature distribution known at time t before a numerical integration is performed. A recomputation of properties take place, based on the just computed temperature distribution and assigned to the middle of the next integration step when the integration is finished.

The inaccuracies introduced in the computation by this quasilinar mode is small, when the time and temperature depenaence is weak or time steps are kept small. Experience has shown, that the quasilinar mode gives negligible errors in the case of heat conductivity, heat capacity, thermal emmissivity or decay heat production. The method may introduce big errors in the case of heat transfer coefficients, and for that purpose the time step is computed from the change of the heat transfer coefficients as discussed in section 4.2.2.

The evaluation of properties is shown at fig. 8 in the case of heat conduction in solids and in fig. 9 for heat conduction between a coolant channel and a solid. The idea behind the figures is:

For a single node, temperature and material properties are assigned to levels along the time axis. Information is created, where

it is marked with a small circle. The arrows indicate the functional relation ship between temperatures and properties. Horisontal arrows are restricted to pure time dependence.

Remarks to fig. 10

The local heat conductivity in radial and axial direction is computed at time t + 1/2 Δt, as functions of node temperature T. This information is combined with similar information from the four neighbouring nodes to give the effective conductivities KR-KZ. Only KR = KR (CONR(T)) and KZ = KZ (CONZ(T)) is shown. The heat added to the node in the time step Δt is determined at time point t + 1/2 Δt.

Remarks to fig. 11

The heat transfer coefficient may be a function of many parameters among which are pressure, coolant temperature, surface temperature, mass flux and heat flux. The heat transfer coefficient associated with the time Δt is a constant mean value at the point in the program loop, where the recomputation of properties takes place.

The local properties of the node are combined with h (t, T_s) and corresponding local properties from the three neighbouring solid nodes to give the effective conductivities. For the sake of simplicity only the computation of KR (CONR(T)), h (t, T_s)) and KZ (CONZ(T)) are shown, and the unlinear effect of thermal radiation between opposite surfaces is also excluded. The surface temperature T_s at t + Δt is computed from the new T distribution and the radial effective conductivity assigned to t + 1/2 Δt.

6. INITIAL TEMPERATURES

DINO has an option for steady state temperature computation. The steady state temperature distribution in the fuel rod and the steady state heat transfer coefficients along the channel must be available for the programme as initial values, before a transient

Heat conduction in solids

Computation of time and temperature dependent parameters before an integration step

Node temperature :	T
Effective radial conductivity:	KR
Effective axial conductivity :	KZ
Node heat capacity :	CP(T)
Heat production in node :	Q(t)
Node axial heat conductivity :	CONZ(T)
Node radial heat conductivity:	CONR(T)

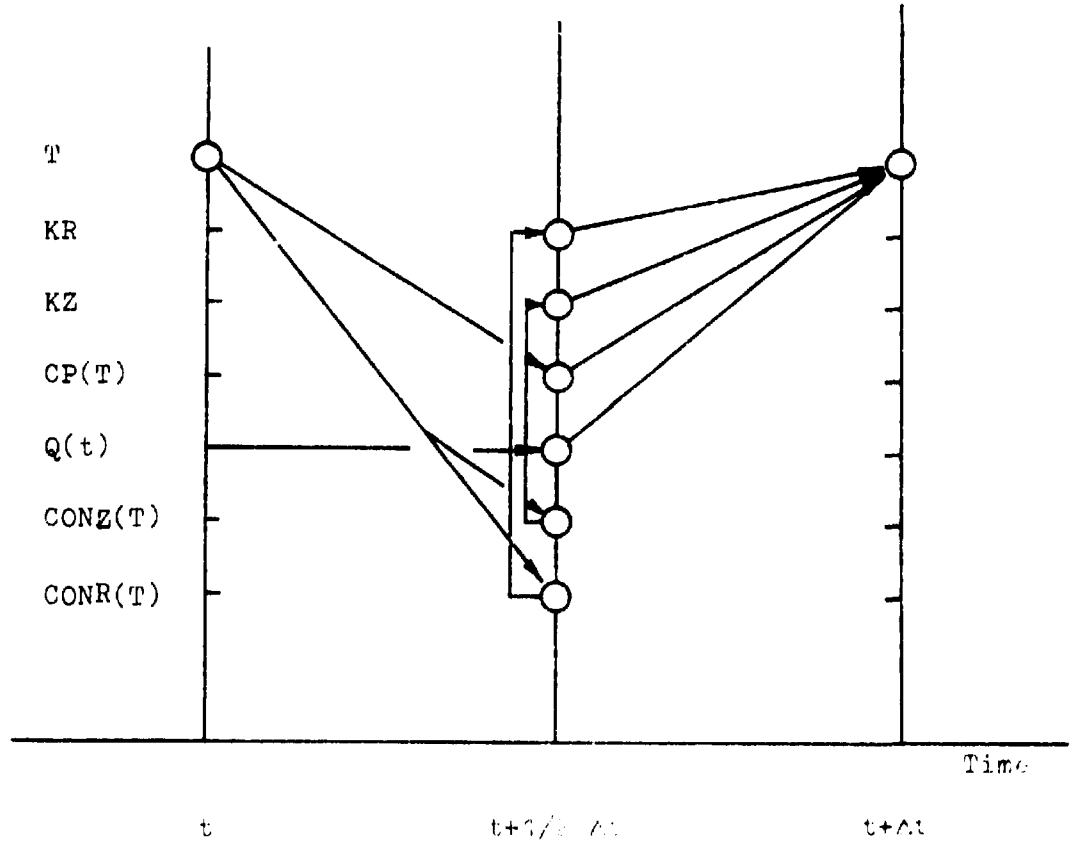

Fig. 10

Heat conduction between a coolant and a solid

Computation of time and temperature dependent parameters before an integration step

Solid node temperature	:	T_N
Effective radial conductivity	:	$KR(T_N, h)$
Effective axial conductivity	:	$KZ(T_N, h)$
Solid node heat capacity	:	$CP(T_N)$
Solid node axial conductivity	:	$CONR(T_N)$
Solid node radial conductivity	:	$CONZ(T_N)$
Heat prod. in solid node	:	$Q(t)$
Heat transfer coefficient	:	$h(p, t, T_s)$
Pressure in channel	:	$P(t)$
Surface temperature	:	T_s
Coolant temperature	:	$T_c(t)$

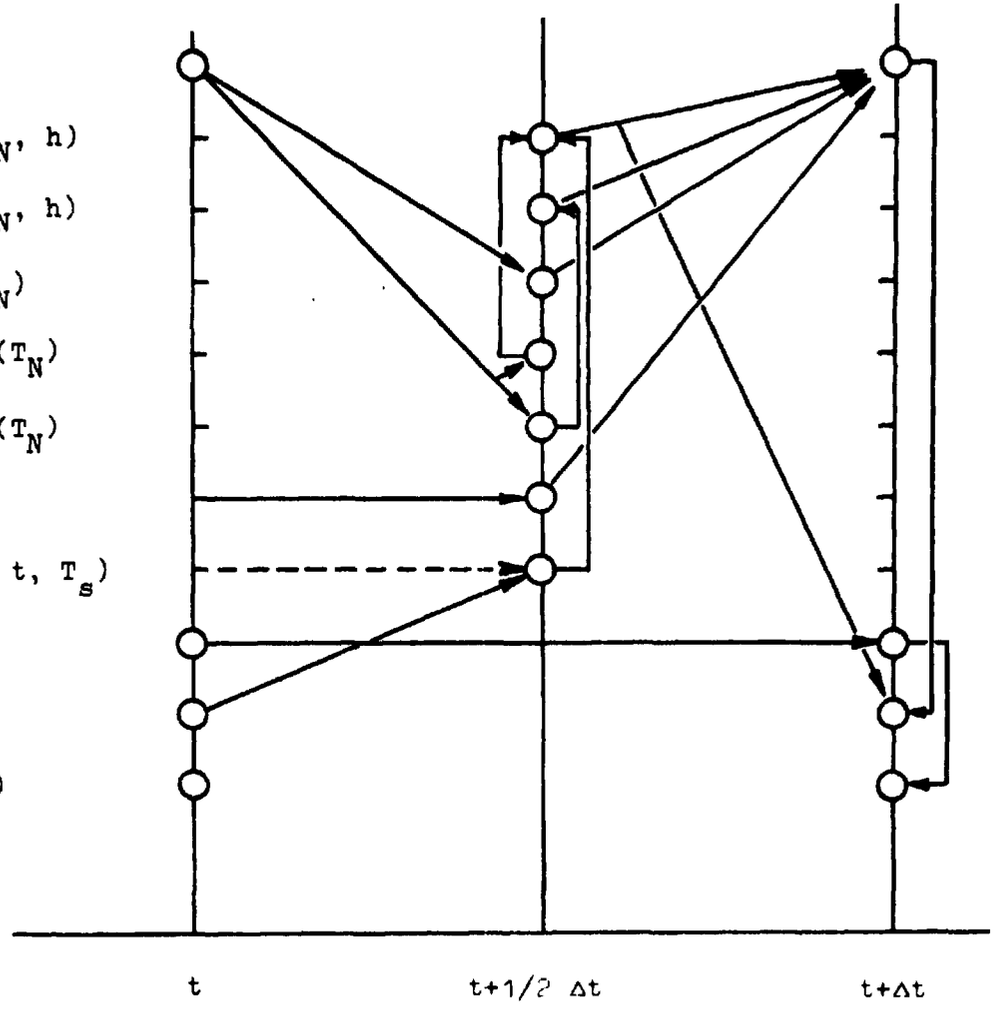

Fig. 11

problem can be treated. The initial values are computed by a transient approach to the steady state by call of all heat conduction procedures, combined with a call to a coolant procedure, written for the steady state heat transfer.

The necessary input informations are besides normal grid and node specifications, axial power distribution, coolant channel mass flux, inlet enthalpy and saturation pressure. The steady state heat transfer is based upon the Dittus-Boelter correlation in the subcooled range and nucleate boiling by Thom in the saturated range. The results of the steady state are punched on data cards by the program, and this card deck must be included in the transient input card deck.

The approach to the steady state is controlled by residuals, computed for each node. Each residual express the ratio between the heat stored in the node in a time increment Δt and the net heat transport from that node in the same time increment.

This relation is expressed by:

$$R = \frac{(T_1 - T_2) \times C_p \times V/\Delta t}{\sum_1^4 KR \times \Delta T \frac{A}{\Delta x} + q_i'''}$$

where

V : node volumen, m^3

C_p : heat capacity, Joule/m^3 ^oC

Δt : time increment, sec.

T_1-T_2: node temperature change in the increment Δt, ^oC

KR : effective conductivity, Watt/m ^oC

ΔT : temperature difference between considered node and its neighbours, ^oC

$A/\Delta x$: ratio heat conduction area, node distance, m

q''' : heat generation, Watt/m^3

7. TEST OF THE PROGRAMME

A test of correctness of a computer-programme of the DINO-type is normally rather difficult and time consuming, due to the complexity of the programme structure. There are normally two basic ways of programme verification to be followed:

1) Two programmes of similar structure may be compared, using a well defined test example. Correspondence between computed results obtained from the test-example gives a relative check of the correctness of the computations.

2) A well defined and well documentated experiment may be used to obtain an absolute check of the computations, when the programme is used to simulate the experimental results.

These two methods have the basic disadvantage, that a succesfull comparison do not prove, that the programme can be released for production. Many test-examples will in nature be outside the original scope of the programme and such a test may stress features of the programme structure, which may only be of minor importance during production runs.

It has not been possible to perform a test, like one of the above mentioned, at the present state of the development of DINO, mainly due to lack of proper experimental data. A carefull investigation of lineprint output and plotter cutput, resulted in corrections of some errors. In general the results from a computation are assumed to be fair, if the shapes of the curves are smooth. Smooth curves indicate, that the deviation with respect to time is continous. The continuity of the derivatives is in general sensitive to unlinearities. Large time steps will cause discontinuities in the derivatives, but a correct programme structure will increase the smoothness of the curves, by decreasing time steps.

To obtain a preliminary analytical experience, we applied the programme to the core heat up problem in the Oyster Creek reactor. The fuel temperature history was compared to corresponding fuel temperatures presented in /10/ fig. 4. The comparison gave identical temperatures approximately 10 sec. after the start of the accident, though we are missing exact information of the Oyster Creek thermal-hydraulic quantities.

The total lineprint output from DINO is huge and very time consuming to produce and investigate. Therefore DINO uses computer plotter procedures to a high extend reducing the manual work of hand plotting. The basis for the wide use of plotting procedures is an accurate graphical representation of the results. The curves produced by DINO is created from a straight line method. Before the results from DINO is plotted, a monitoring of the time distance between successively computed results takes place. The minimum distance is chosen to be 0.05 sec. The programme selects results for plotting from their time arguments, when the time increment exceeds 0.05 sec.

The straight line method means that the plots consist of straight lines between the selected points. The straight lines are by the plotter system divided into basic plotter steps /11/ that is 0.1 mm in the vertical and horisontal directions and 0.14 mm in the direction of the diagonal.

8. ANALYTICAL EXPERIENCE

The ability of the programme to describe the thermal response of a fuel rod due to a loss of coolant accident, has been tested on a boiling water reactor of the Oyster Creek type.

The blow down of the reactor has been computed by the BRUCH-S, and relevant data have been stored on a magnetic tape, for further processing in DINO. A double ended rupture in the recirculation line, next to the lower plenum, is considered. The reactor is operated normally at full power, when the rupture occurs. Full power is assumed in 0.4 sec. after the accident and a decay curve determines the reactor power during the rest of the blow down.

The fuel rod considered is a corner rod in the hottest channel of the reactor. The rod is divided into 50 axial levels, to obtain a detailled picture of the influence of the axial power distribution on the thermal response.

Each level of the rod is radially divided into 4 fuel nodes and 1 cladding node. The heat transfer and burnout correlations described in section 4.2.1. are applied in the following conservative way. When burnout is indicated for a level, no further calculation of the burnout takes place at this level. The burnout indication is retained in the succeeding calculations.

9. RESULTS

The results of the runs with BRUCH-S and DINO are shown at figures 12 - 20. Figure 12 shows the pressures versus time in different parts of the reactor due to the accident. When the accident starts the pressure in the lower plenum falls drastically due to the subcooling in this volumen, while the pressures in the core and the steam dome decreases moderately. These pressure differences cause the flow oscillations through the core.

Figure 13 shows the mean mass flow through the core. It should be noticed, that the flow direction is reversed several times. Immediately after the rupture, the flow stagnates due to the heavily decreased lower plenum pressure and burnout takes place.

Figure 14 shows the relative axial power distribution in the hottest fuel element. The rod is divided into 50 axial levels to take into account the axial variation of the power. The numbers on the curves in the figures 15 - 19 correspond to these axial levels. Level 50 is top of fuel rod, and level 34 is the maximum power level, approximately 1.05 m below the top. Level 20 is app. 2.10 m below the top of the fuel rod.

Figure 15 shows the rod center temperature versus time. The temperatures are constant 0.4 sec. after the accident due to the reactor power curve. The center temperatures decrease, when the power decreases, and are not influenced by the channel.

Figure 16 and 17 show the rod surface temperatures versus time. Figure 16 is obtained with an accuracy i.e. band width of 0.01, while figure 17 shows the results with an accuracy of 0.04.

Some oscillations due to truncation errors is introduced in the plots, but it should be noticed, that the end temperatures of both figures are identical. The increase in temperatures immediately after the start of the accident is the result of burnout.

Figure 18 shows in semi logarithmic scale the computed heat transfer coefficients versus time. Burnout takes place app. 40 msec after the rupture due to the flow reversing immediately after the accident. The heat transfer mechanism is not allowed to return to nucleate boiling, so throughout the computation the curves represent transition and film boiling heat transfer. Each time the flow reverse, the heat transfer coefficients fall to a low value due to flow stagnation.

Figure 19 shows the rod surface heat flux versus time. Low flux levels are identical to low heat transfer coefficients, see fig. 18. The plots are, however, obtained with a band width of 0.08, why some ripples can be observed. As an increase in the heat flux is observed in the first few msec. a detailled description is given in figure 20. The plot is restricted to level 34.

Four runs are shown - two with an accuracy of 0.08 and two, applying a band width of 0.01. In these runs the transition exponent (see section 4.2.1) has been used as a parameter, restricting the lower limit values of n to 0.01 and 0.1.

A lower limit of 0.01 corresponds to a heat transfer during the early parts of transition of 90% of nucleate boiling rates, while the lower limit 0.1 only gives a transition max. heat transfer rate of 50% of nucleate boiling.

The increase in the surface heat flux may be explained by the larger increase in the temperatures than the decrease in the heat transfer coefficient. This effect is rather short and it is only seen in high power levels.

REFERENCES

1. Karwat, H.,
A non-linear multinode study for a boiling water reactor.
MRR 34, Institut für Mess- und Regelungstechnik, München (1967).

2. Andersen, Jens, Abel-Larsen. H.,
REMI/HEATCOOL
A Computer Programme for Calculation of Core Heat Up and Emergency Core Cooling Transients.
(To be published).

3. Abel-Larsen, H., Lolk Larsen, M.,
Heating in a reactor fuel rod under transient conditions.
Part I. Heat conduction program.
Risø-M-1391 (1971).

4. Peaceman, D.W., Rachford, H.H. Jr.,
The numerical solution of parabolic and elliptic differential equations.
J. Soc. Indust. Appl. Math. 3,
No. 1, 28-41 (1955).

5. TEMPDIST, an ALGOL program for calculation of temperatures in a UO_2 fuel rod.
Cortzen, F., List, F., Rathmann, O.,
Risø-M-944 (August 1969).

6. Thom, J.R.S. et al.,
Boiling in Subcooled Water during Flow up Heated Tubes or Annuli.
Proc. Instn. Mech. Engrs. 1965-1966.
Vol. 180, Part 3C (1966).

7. Bertoletti, S. et al.,
Heat transfer crisis with steam-water mixtures.
Energia Nucleare, Vol. 12, No. 3 (1965).

8. Parker, J.D., Grosh, R.J.,
Heat transfer to a mist flow.
ANL-6291 (1961).

9. Groeneveld, D.C., Revised by Moeck, E.O.,
An investigation of heat transfer in the liquid deficient regime.
AECL-3281 (1969).

10. Docket 50219-143,
Oyster Creek unit I, Amendment no. 67.

11. Use of the digital plotter in Algol programs on B6500, by P. Voss.
Risø-M-1366 (April 1971).

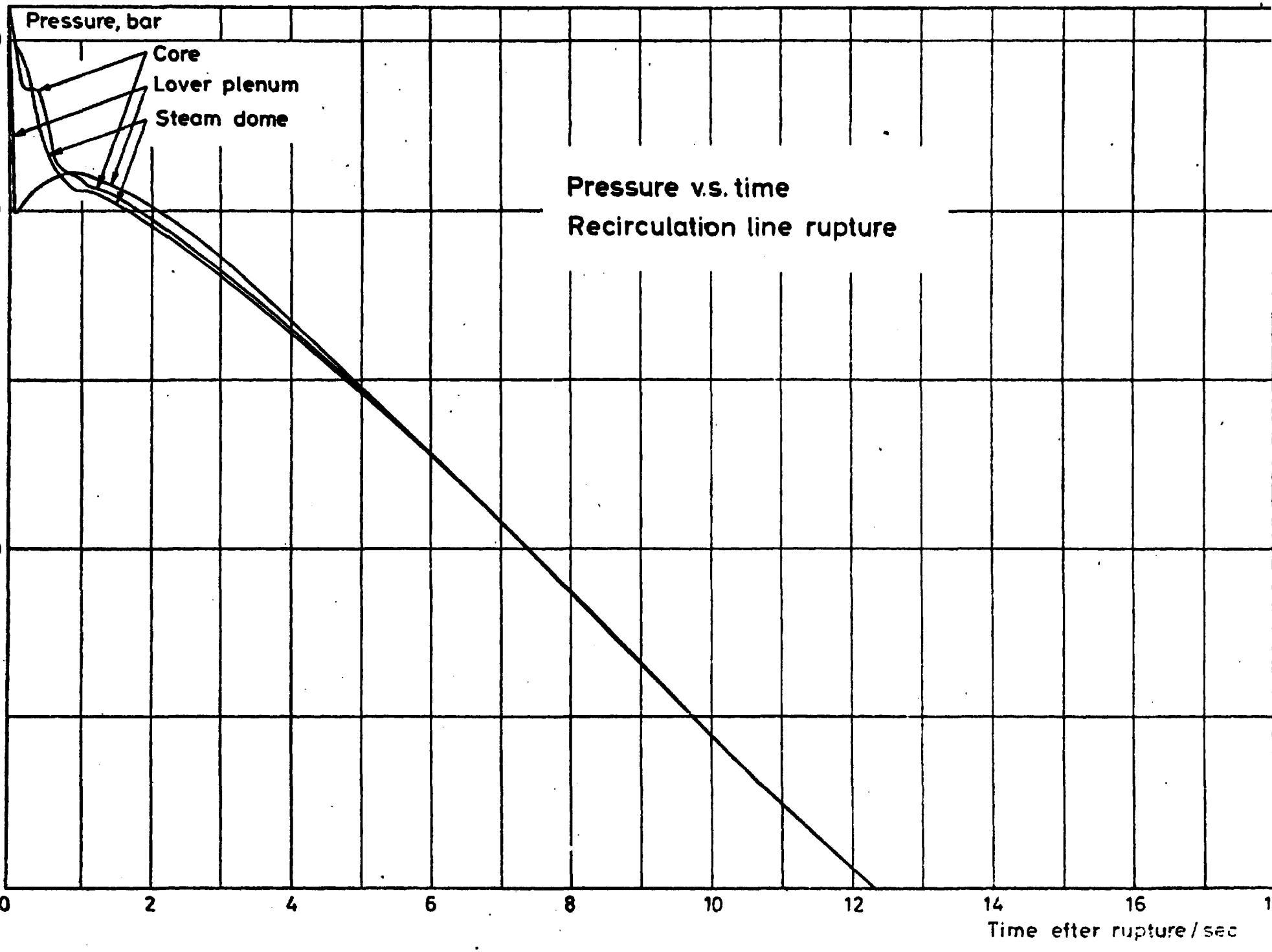
Pressure, bar
Core
Lover plenum
Steam dome
Pressure v.s. time
Recirculation line rupture
60
50
40
30
20
10
0
2
4
6
8
10
12
14
16
Time efter rupture / sec

Fig. 12

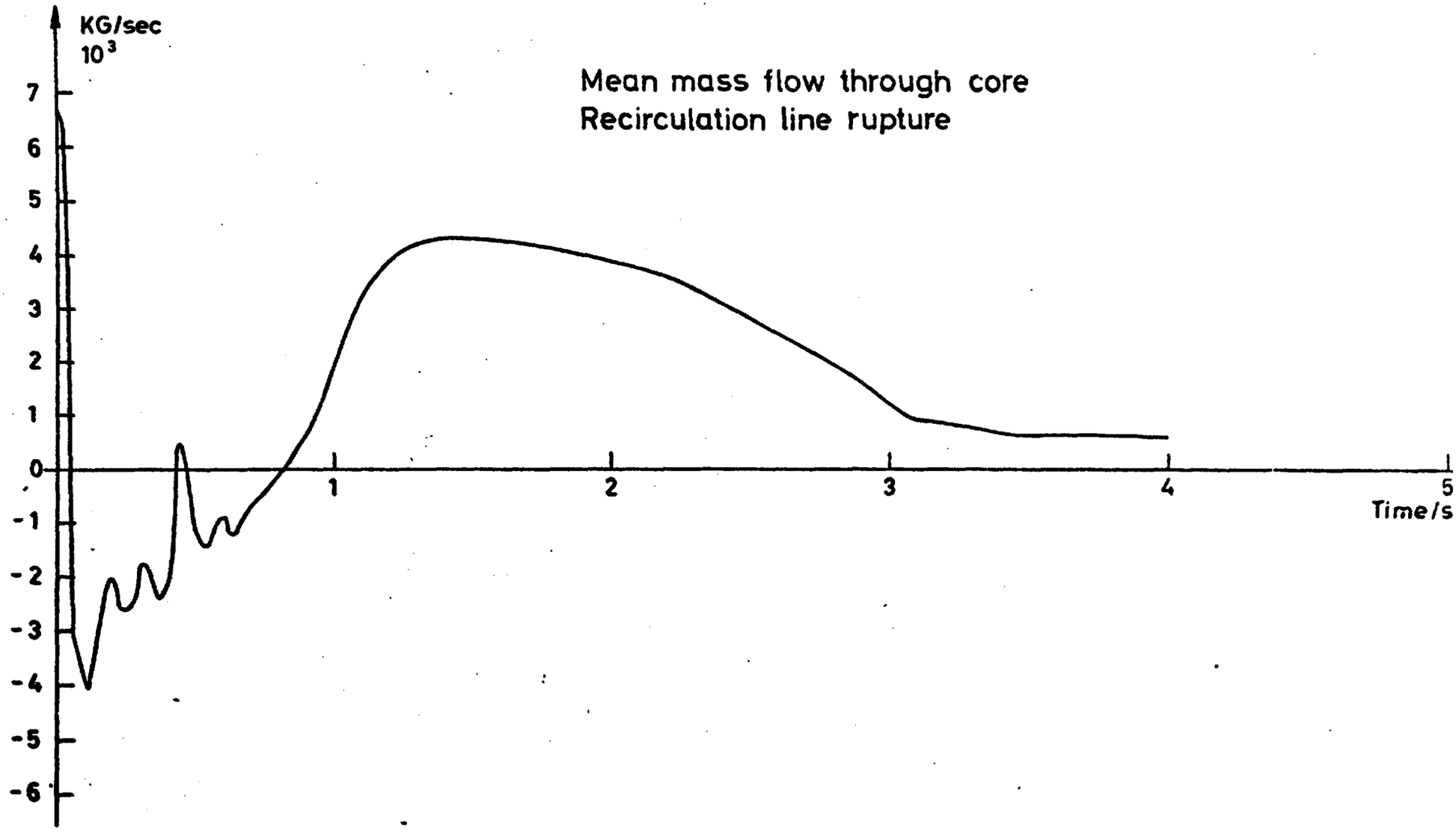
KG/sec
10³
7
6
5
4
3
2
1
0
-1
-2
-3
-4
-5
-6
1
2
3
4
5
Time/s
Mean mass flow through core
Recirculation line rupture

Fig. 13

Axial power distribution
Form factor 1.4

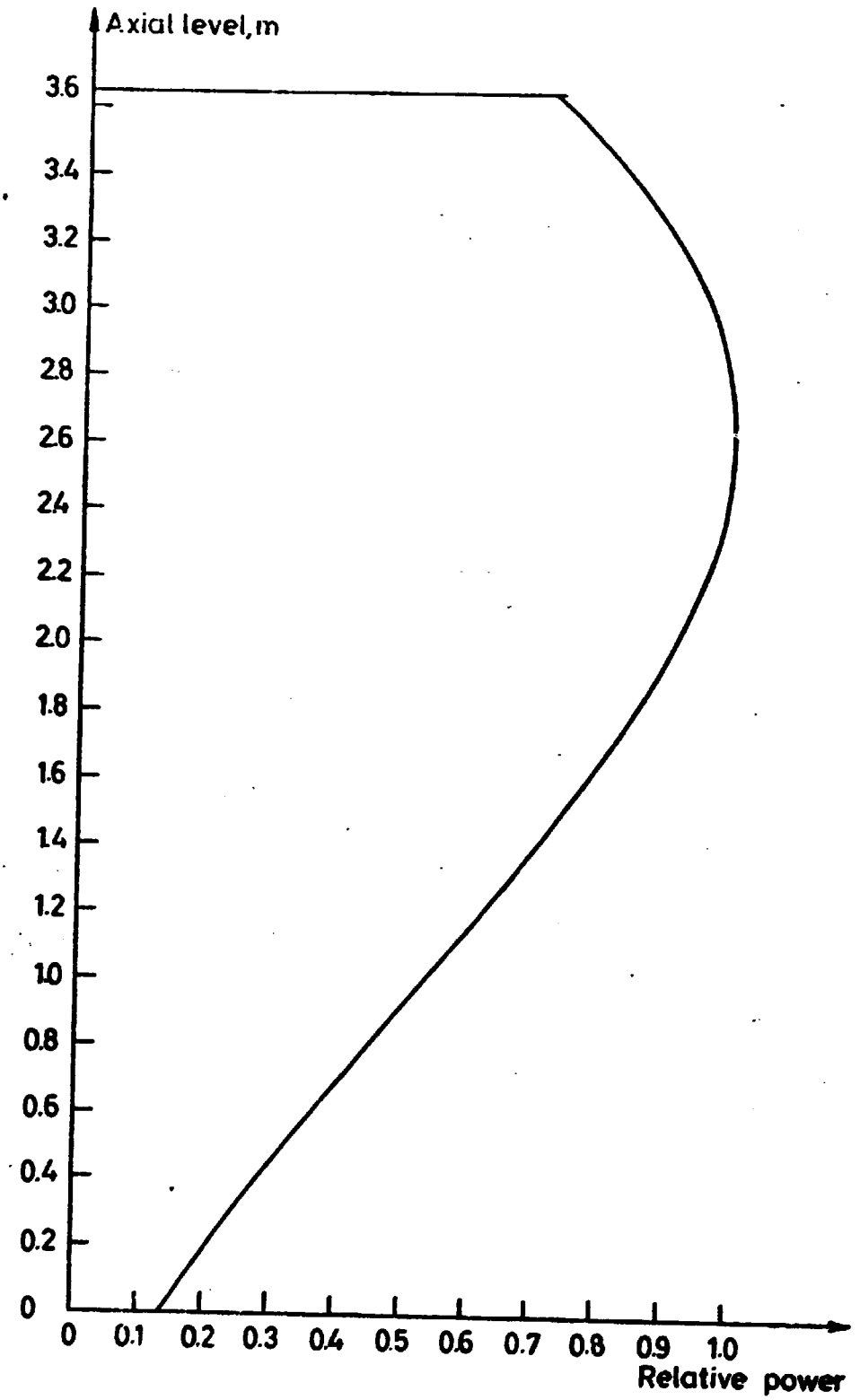

Fig. 14

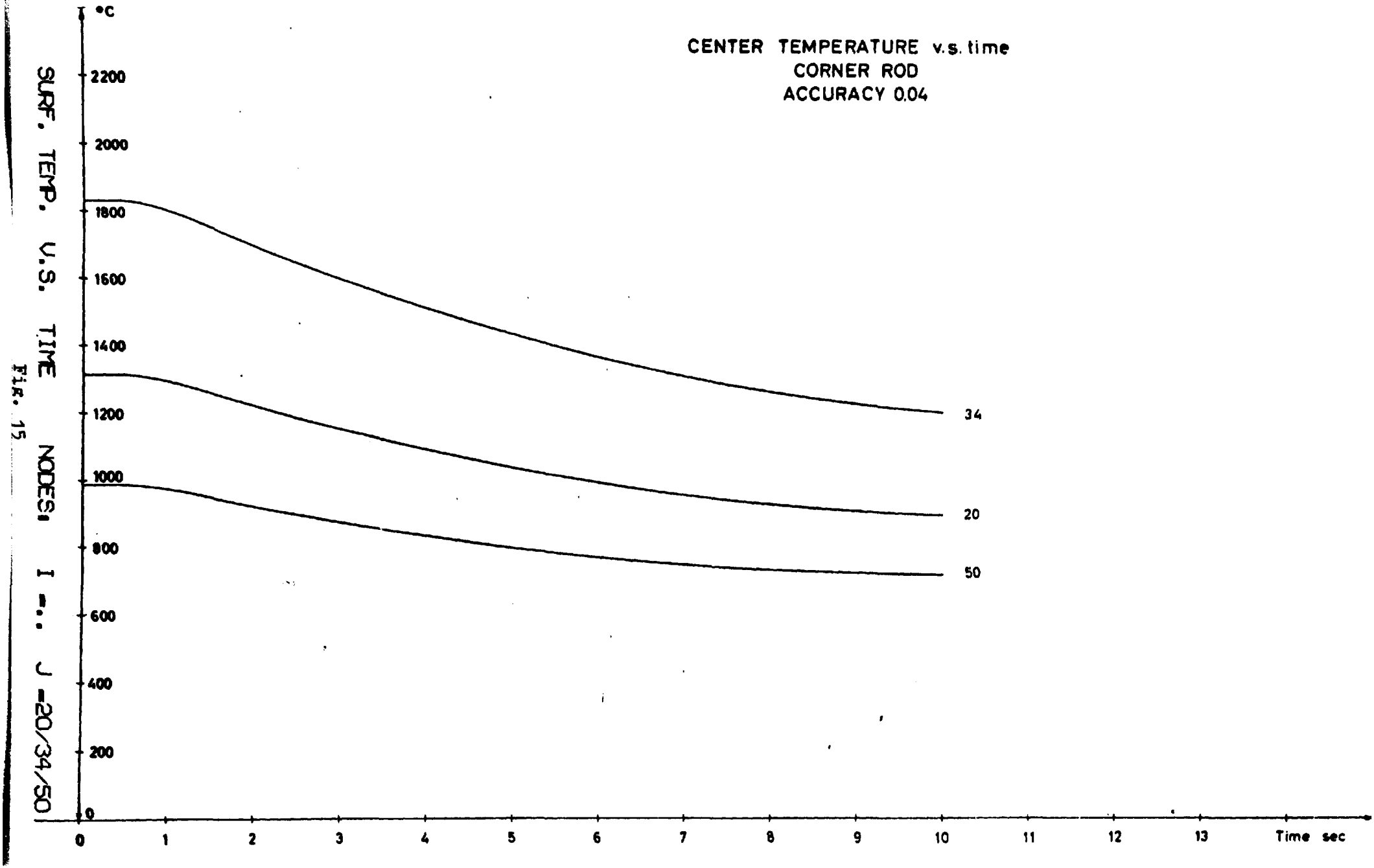
CENTER TEMPERATURE v.s. time
CORNER ROD
ACCURACY 0.04
°C
2200
2000
1800
1600
1400
1200
1000
800
600
400
200
0
SURF. TEMP. V.S. TIME NODES: I =.. J =20/34/50
34
20
50
0
1
2
3
4
5
6
7
8
9
10
11
12
13
Time sec

Fig. 15

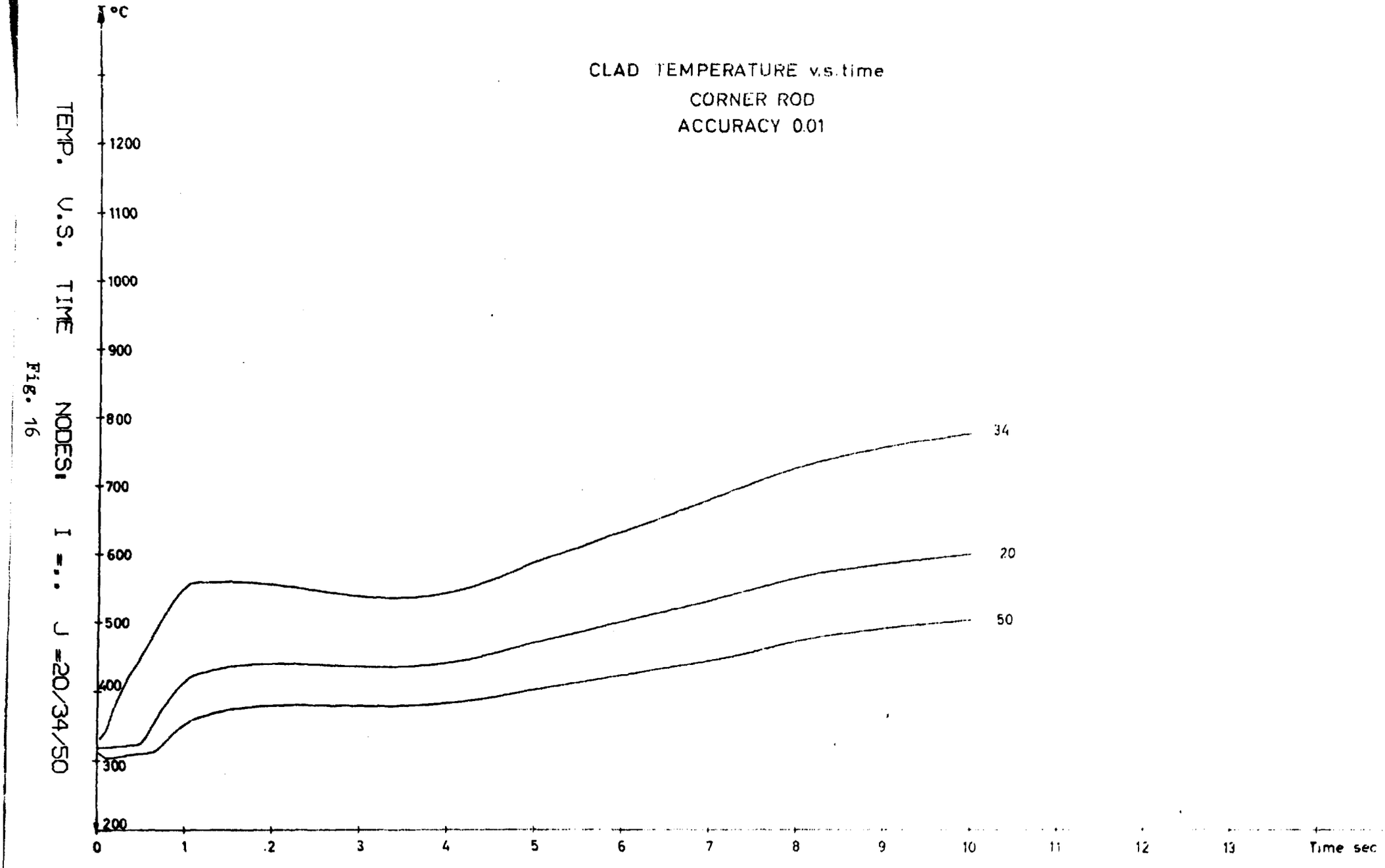
CLAD TEMPERATURE v.s.time
CORNER ROD
ACCURACY 0.01
°C
1200
1100
1000
900
800
700
600
500
400
300
200
0
1
.2
3
4
5
6
7
8
9
10
11
12
13
Time sec
34
20
50
TEMP. V.S. TIME NODES: I =.. J =20/34/50

Fig. 16

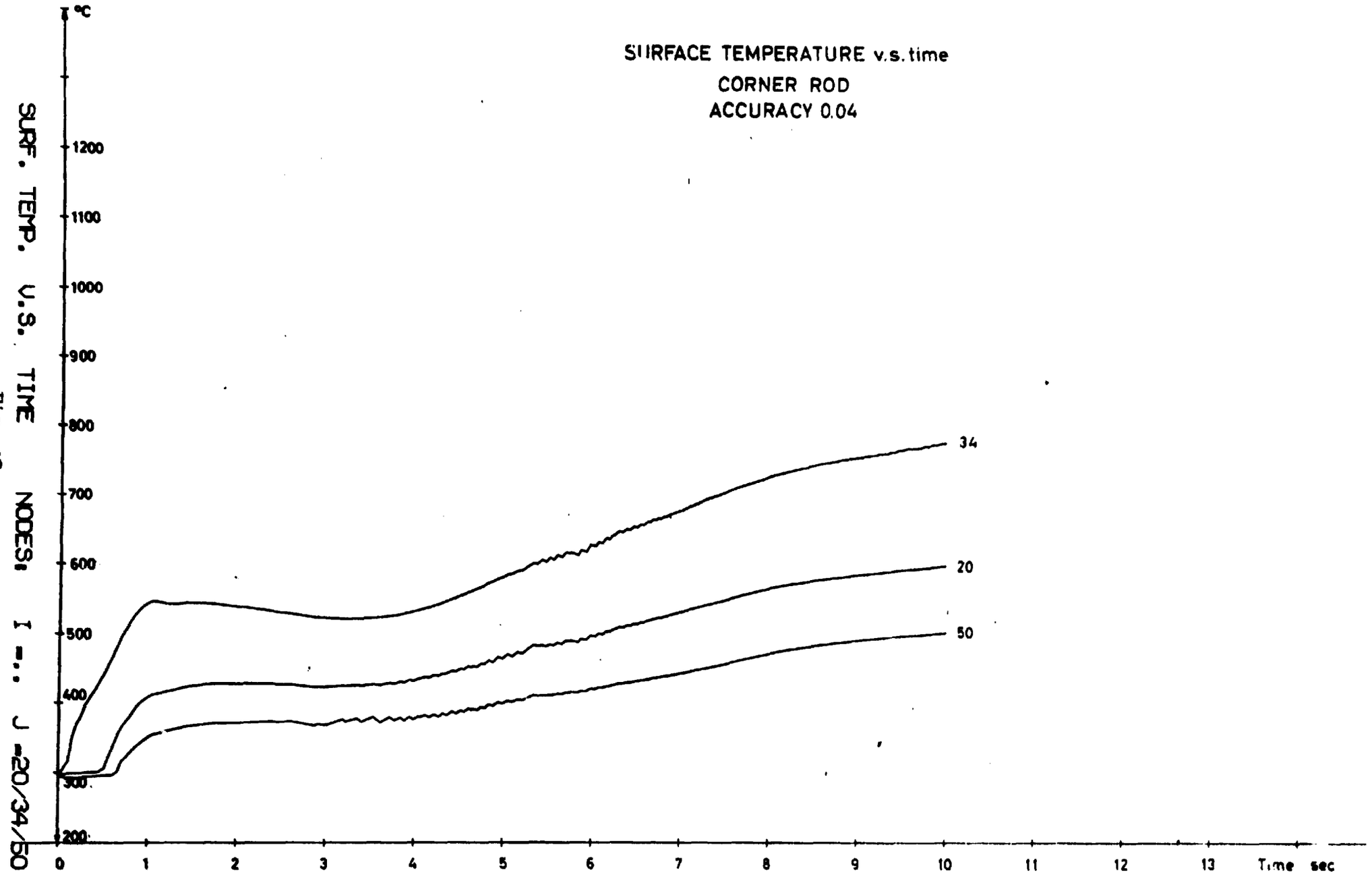
SURFACE TEMPERATURE v.s. time
CORNER ROD
ACCURACY 0.04
SURF. TEMP. V.S. TIME NODES: I = ... J = 20/34/50
T °C
1200
1100
1000
900
800
700
600
500
400
300
200
0
1
2
3
4
5
6
7
8
9
10
11
12
13
Time sec
34
20
50

Fig. 17

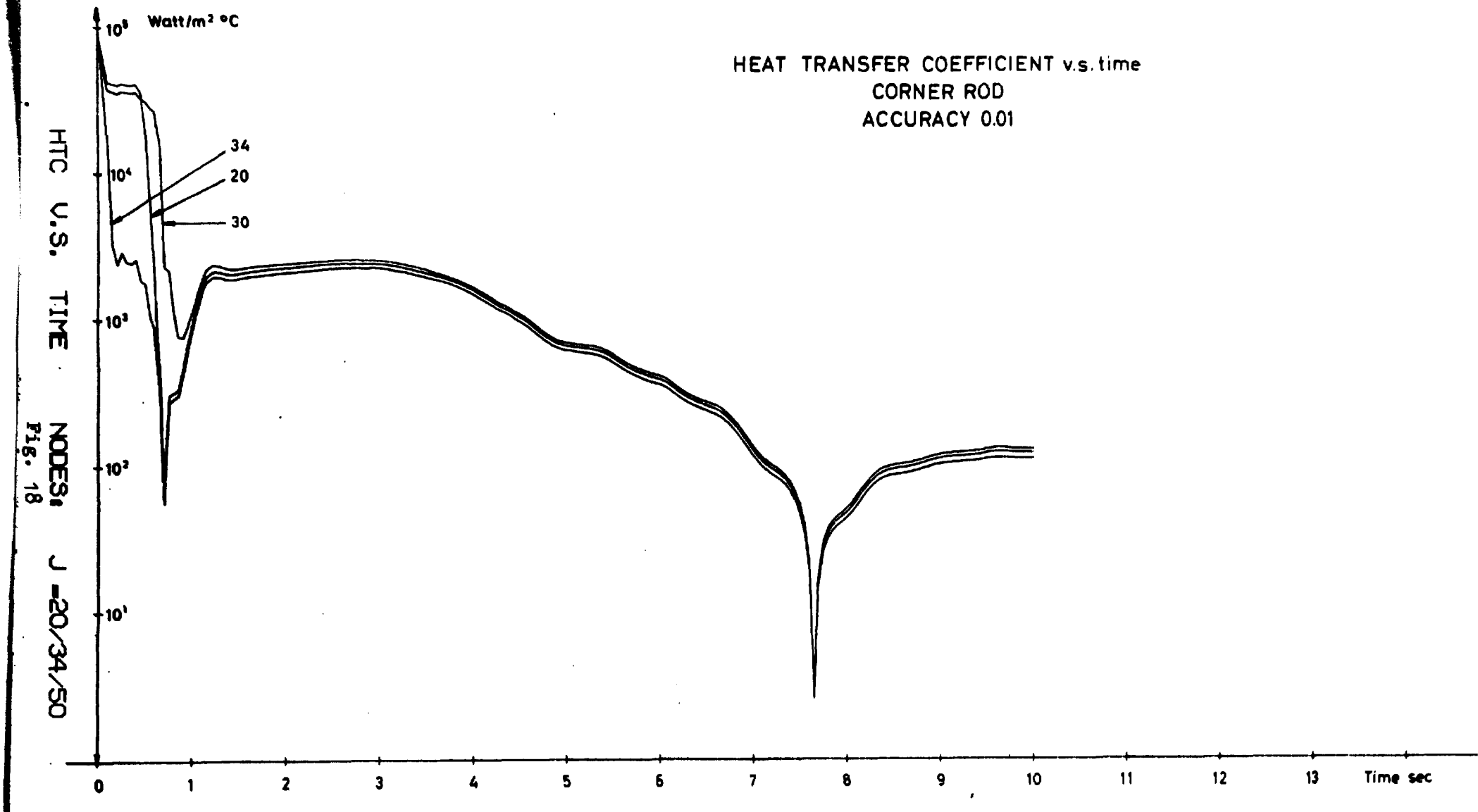
HEAT TRANSFER COEFFICIENT v.s. time
CORNER ROD
ACCURACY 0.01
HTC V.S. TIME NODES: J =20/34/50
Watt/m² °C
10⁵
10⁴
10³
10²
10¹
34
20
30
0
1
2
3
4
5
6
7
8
9
10
11
12
13
Time sec

Fig. 18

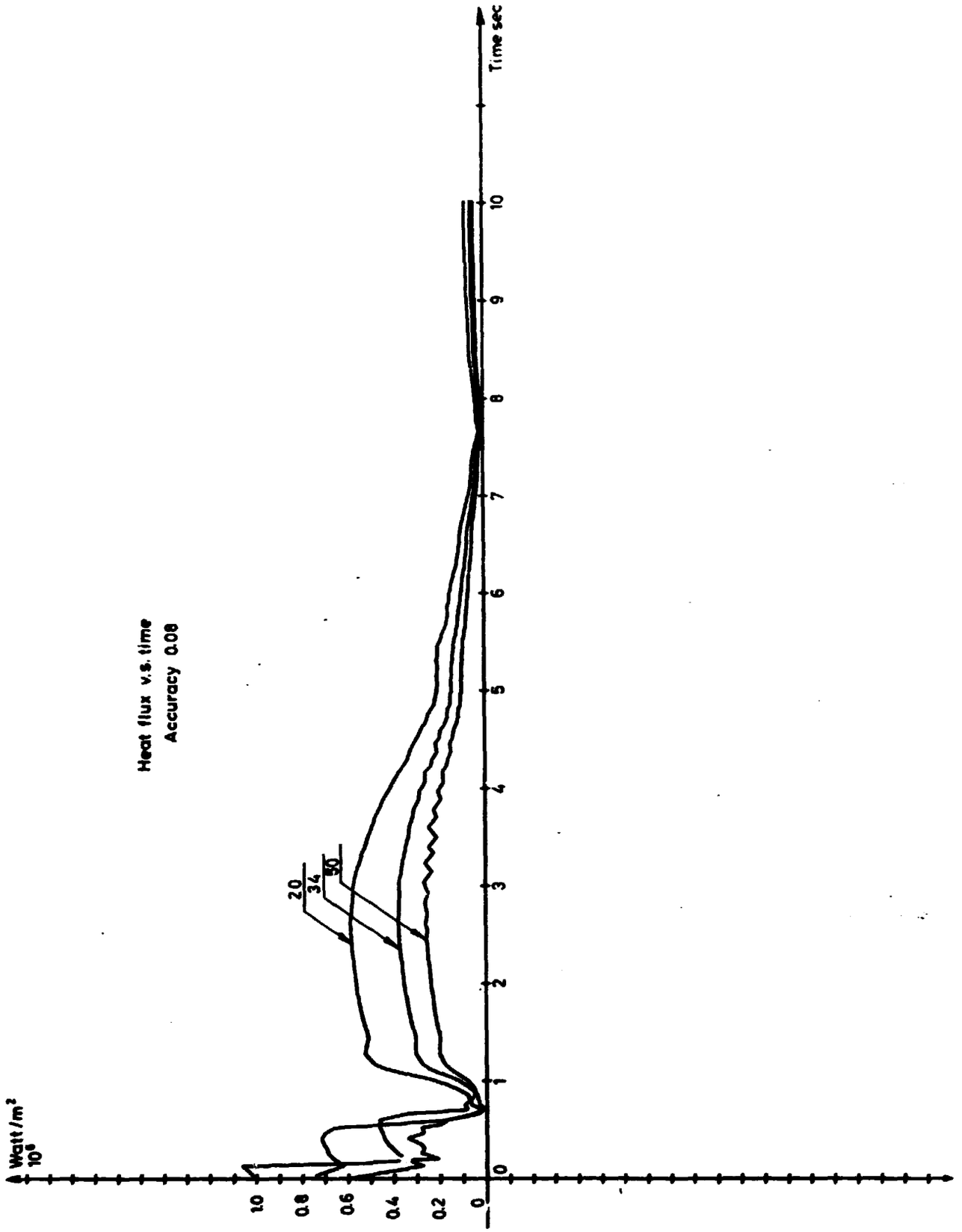

HEATFLUX V.S. TIME NODES: I= ..J= 20/34/50

Fig. 19

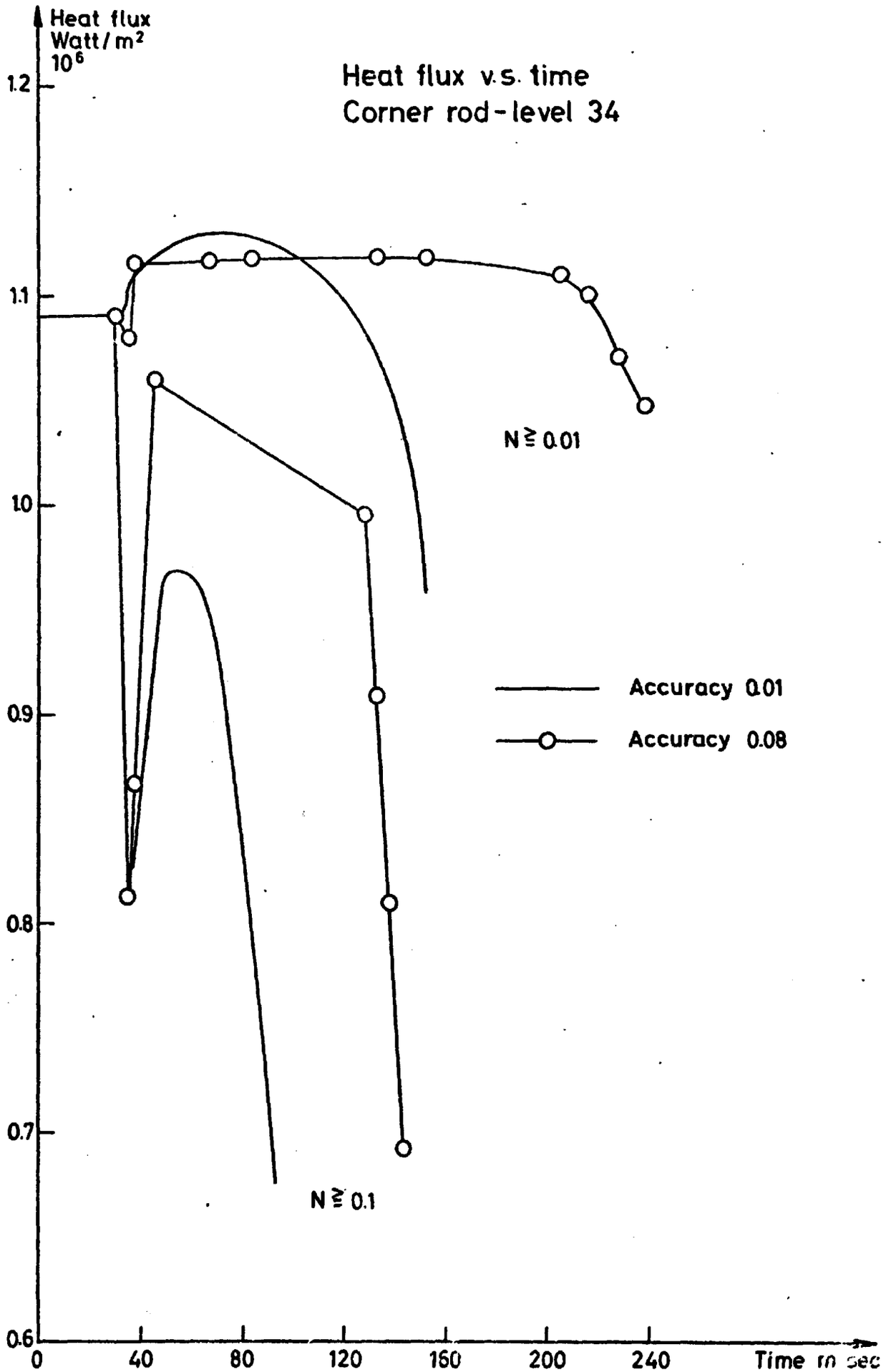
Heat flux
Watt/m²
10⁶
Heat flux v.s. time
Corner rod - level 34
1.2
1.1
1.0
0.9
0.8
0.7
0.6
N ≧ 0.01
N ≧ 0.1
Accuracy 0.01
Accuracy 0.08
0
40
80
120
160
200
240
Time in sec

Fig. 20